

Review

Ion mapping in plant cells – methods and applications in signal transduction research

Werner Roos

Deptartment of Cell Physiology, Institute of Pharmaceutical Biology, Martin-Luther-University Halle, Kurt-Mothes-Str. 3, 06120 Halle (Saale), Germany E-mail: roos@pharmazie.uni-halle.de; Fax: +49-345-5527006

Received: 26 May 1999 / Accepted: 2 August 1999

Abstract. This review covers both methodical aspects and actual applications of ion imaging techniques in plant cell signal research. The methodological section explains the basic principles of fluorescence ion imaging, the impact of modern developments in fluorescence microscopy and introduces the most important fluorescence probes including aequorin and other photoproteins. It critically comments on loading strategies, intracellular compartmentation of probes and calibration procedures. The second part compiles actual research areas where the application of ion imaging procedures has gained substantial achievements and helped to establish new concepts of calcium- and pHdependent signalling. Examples comprise the hormonal control of stomatal movements, effects of gibberellic and abscisic acids in aleurone cells, elicitation of phytoalexin production, cytosolic pH and cell development, and signatures of Ca²⁺ as a universal signal in plant cells.

Key words: Ca²⁺ mapping – Cellular signal transduction – Confocal ion topography – Fluorescence ion imaging – Ion compartmentation – pH mapping

Introduction

The dynamic compartmentation of cellular ions and its involvement in metabolism and signalling are basic features of life. In the last decade, with the advent of new fluorescent probes and powerful imaging techniques the visualization and quantification of ion concentrations in eukaryotic cells has become a main goal of biological fluorescence microscopy. Today, many cell types can be prepared and examined with a minimum disturbance

Abbreviations: ABA = abscisic acid; AM = acetoxymethyl; GA_3 = gibberellic acid; GFP = green fluorescent protein; IP_3 = inositol (1,4,5) trisphosphate; pH_{in} = intracellular pH; pH_{cyt} = cytosolic pH; abbreviated names of fluorescent probes are compiled in Tables 1 and 2

of the cellular organization to yield maps that show the topography of various ion activities, including their gradients and dynamics, with the resolution of light microscopy. Due to the high rigidity of plant cells and tissues and their content of strongly refractive or fluorescent structures (cell wall, cuticle, chloroplasts) the progress of ion mapping techniques was retarded compared to their fast distribution in animal cell sciences. Persisting problems with the loading and cellular compartmentation of ion indicators have been addressed by developing a variety of probes and experimental protocols and some of them can be expected to be circumvented by the transgenic expression of indicator proteins. Altogether, remarkable achievements have been made in the recent past that promise an increasing impact of ion imaging on major areas of green-cell biology.

The basic methodological aspects of quantitative fluorescence ion imaging have actually been reviewed by Mason et al. (1999). Several reviews compile the strategies, limitations and practical aspects of Ca²⁺ imaging, mainly in animal cells (e.g. Nucitelli 1994; Schild 1996; Opas 1997). A methodologically oriented approach to Ca²⁺ and H⁺-mapping in plant cells, including experimental protocols, is given by Fricker et al. (1993, 1999). The present paper attempts an updated overview of basic methodology, capacities and limitations of ion imaging in plant cells followed by a compilation of actual research areas of plant cellular biology where imaging procedures have helped to gain substantial achievements.

The principles

Basic procedures

Ion imaging by fluorescence microscopy is based on fluorescent probes that accumulate inside cells and change their fluorescence properties when bound to distinct ions. Such alterations can be (i) shifts in the excitation and/or the emission spectrum (ratiometric probes), (ii) changes in the fluorescence intensity at one distinct wavelength (single-wavelength probes) and/or (iii) changes in the lifetime (related to phase angle and modulation) of the emitted light. The fluorescence images obtained by a video camera or photomultiplier are then digitised and assayed by image analysis.

Up to now, ratioing of fluorescence intensities has been the method of choice in ion imaging. Cells loaded with ratiometric probes are examined at two different bands of either excitation or emission wavelengths that detect (exclusively or preferentially) the fluorescence of either the ligand-bound or -unbound form of the probe. A pair of fluorescence images is thus obtained and the intensities of each data point (pixel) are ratioed. The resulting ratio image represents the fluorescence changes caused by ligand binding only and thus maps the distribution of the desired ion. The ratioing principle eliminates any heterogeneities of fluorescence that occur in either of the paired images as nonuniform dye accumulation, leakage of the probe, photobleaching, thickness of specimen, or inequalities of the fluorescence detection.

The maximum dynamic range of the probe is exploited by dividing signals obtained at two wavelengths with opposite ion dependence of fluorescence. Alternatively, if the spectrum contains an isosbestic point, i.e. a wavelength at which the fluorescence is independent of the ion concentration, this can be selected to obtain one of the paired images which then mirrors the distribution of the probe.

Single-wavelength probes, which react to ion binding with changes in fluorescence intensity but no spectral shift, yield ion maps that are originally not corrected for the above-mentioned sources of error and hence allow no exact quantitation. Most Ca²⁺ probes excitable by visible light belong to this group. Their use appears justified and is indispensable if time series of strong Ca²⁺ shifts are to be visualized without exposing the cells to UV irradiation, especially by confocal laser scanning microscopy where visible-light laser sources are in routine use, e.g. during fertilization of sea urchin eggs (Gillot and Whitaker 1993) or in abscisic acid-(ABA)stimulated guard cells (Irving et al. 1992). Attempts to correct ion maps for the heterogeneous distribution of a single-wavelength probe have been made by two-dyerationing, i.e. the cellular distribution of the ion probe is estimated from the fluorescence image of another, easily detectable dye that is assumed to display similar patterns of distribution. For example, in *Fucus* zygotes Ca²⁺ was mapped by ratioing the image obtained with Calcium Green to another fluorescence image obtained with cSNARF-1, a pH probe which in this case was monitored at a pH-insensitive wavelength (Berger and Brownlee 1993). However, quantitative ratiometric imaging by such dual indicator techniques requires careful determination of the concentration ratio of both dyes in the cell studied: after co-loading of the Ca²⁺ probes Fura-red and Fluo-3 this ratio varied considerably between indivdual (animal) cells (Floto et al. 1995).

Another approach is to divide all images or differences in subsequent images of an experimental series by a

start image (t_0 – or pre-stimulus image), provided that the distribution of the probe, path length and intensity of excitation remain constant throughout the experiment (Neher and Augustine 1992; Gillot and Whitaker 1993, Ehrhardt et al. 1996).

Actually, a more accurate way to use non-ratiometric probes in ion mapping is offered by fluorescence-lifetime imaging, i.e. a method that does not measure local fluorescence intensities but concentration-independent parameters of the emitted light as phase angle or modulation frequency (see below).

Optical resolution of ion maps

In conventional fluorescence microscopy all fluorophore molecules are illuminated that are present within the cone formed by the excitation light (wide-field illumination) and the detector collects both in-focus and out-of-focus light emissions. Therefore, the fluorescence images and the resulting ion maps display a less-defined average of information that is collected throughout the sample depth and thus cannot be attributed to a distinct horizontal plane. With these limits accepted, conventional microscopy and ratio imaging can be used to yield two-dimensional (2D) overviews of ion distribution preferentially in cells or organelles of regular structure, e.g. in yeasts (Slavik and Kotyk 1984), protoplasts (Roos and Slavik 1987) or guard cells (McAinsh et al. 1992, 1995).

The light from out-of-focus parts of the cell causes blurring of fluorescent images, thus obscuring details and complicating the alignment of intensity distributions and derived ion maps with small cellular structures. Both optical methods and image-processing algorithms have been developed to overcome this and other limitations of optical resolution and contrast.

Confocal microscopy. At present, the most-defined images to be used for ion mapping are provided by confocal fluorescence microscopy. In the confocal microscope, the excitation light (a collimated laser beam) and, even more so, the emission light are confined by adjustable pinholes to small volumes that lie along the optical axis. Only the light emerging from focal regions of the specimen passes through the exit pinhole and reaches the photomultiplier detector. By simultaneous scanning of both the illuminating laser beam and the detection point over the specimen a fluorescence image emerges pixel by pixel, thus generating a definable optical section through the cell that contains very little out-of-focus information (Inoué 1990). Different scanning modes are in use that allow maximum scan speeds between 10 and >100 images per second (the latter, however, at lowered spatial resolution); hence, even fast shifts in ion concentration can be monitored (Lipp and Bootman 1999; Mason et al. 1999). Dual excitation as well as splitting of the emitted light into two or more channels with individual wavelength settings allows different modes of ratio imaging immediately after image acquisition. The resolution in the x, y direction, as is determined by the resolution and numerical aperture of the objective, can be further improved by the hardware zoom facility of confocal microscopes and the excellent image contrast. At a magnification of 100× and a zoom factor of 8, the theoretical distance between two resolved pixels is 48 nm; in praxi, cellular structures at 150–200 nm distance can well be resolved. The "depth of field", i.e. the thickness of one horizontal plane that appears to be sharply in focus is, among other factors, strongly influenced by the diameter of the detection pinhole; for an objective of numerical aperture (NA) = 1.4 and at λ = 488 nm it can minimally reach 0.7 µm (Inoué 1990). By stepping the object through the vertical dimension, vertically aligned images can be obtained that may be combined to form three-dimensional (3D) arrays.

Computational approaches. Spherical and photometric aberrations are inherent to all fluorescence imaging procedures, though to different extents and in different proportions (White et al. 1996). Many of them can be corrected for by mathematical approaches that are based on the point-spread function of the microscope, i.e. the 3D shape that is formed by the light emitted by an ideal point source.

Conventional epifluorescence images can be deblurred by subtracting out-of-focus information via deconvolution, a procedure that works with several digitized images taken from the in-focus plane and the neighbouring out-of-focus planes (Agard et al. 1989; Scalettar et al. 1996). Modern algorithms have been invented that minimize the number of images to be collected and at the same time allow a high spatial resolution of 2D or 3D ion maps (Carrington et al. 1995). For ratiometric Ca²⁺ measurements an image-processing scheme based on inverse filtering has been developed that extracts thin optical sections from a single image (Monck et al. 1992).

Confocal and two-photon images (see below) still contain spherical and chromatic aberrations that are due to imperfect alignment of illumination and detection volumes, and the influence of highly refractive cellular structures, especially in thick specimens, and therefore benefit from modelling and eliminating errors by image processing as well (White et al. 1996). Actual developments of both deconvolution software and computing power will soon shorten the processing time to a degree that allows viewing the corrected images in real time.

New methodical developments

In the near future, two promising developments in fluorescence microscopy might substantially improve the applicability as well as the resolution of ion mapping. Although confocal scanning microscopy largely reduces the light input into the specimen compared to conventional fluorescence illumination it still requires the excitation volume to be larger than the detection volume. Hence, the photostress exerted by the excitation light also includes some out-of-focus areas along the illumination path.

Two-photon counting. Two-photon counting allows the excitation volume to be kept as small as the detection volume and to be reduced to the sub-femtoliter range. This volume is determined not by a pinhole but by the focus section of a laser beam in that the photon density is high enough to allow the simultaneous absorption of two photons by the same fluorophore molecule. In this area, a fluorescent probe can therefore be excited by photons that contain approximately half the energy required for one-photon excitation. Practically, near infrared (NIR) illumination is used instead of UV or blue illumination to induce visible fluorescence. The central problem is to meet the required photon flux densities without causing thermal damage to the probe. Therefore, excitation occurs by ultrashort NIR pulses of pico- or femtosecond duration, a frequency around 100 MHz and average power levels in the 5- to 10-mW range. In cells that do not contain NIR-absorbing constituents (which is often the case), out-of-focus areas are not exposed to photostress nor do they emit fluorescence (König et al. 1996a; Sako et al. 1997). A direct comparison of two-photon laser scanning and UV-confocal laser scanning microscopy has been performed, e.g. in a study of Ca²⁺ imaging in cultured mouse keratinocyte cells, with the probe Indo-1 (Sako et al. 1997). Though the two-photon excitation required a much higher laser power (12 mW at 710 nm) than UV excitation (0.09-0.18 mW at 351 nm) for a similar signal response, it exhibited a lower rate of photobleaching and a much lower background level that led to a higher image contrast. The Ca²⁺ maps obtained by two-photon excitation were less sensitive to autofluorescence and the number of scanning series. However, in more-sensitive cells the thresholds for non-destructive energy input appear to be much lower (1–5 mW; König et al. 1997). In general, conditions for two-photon microscopy need to be carefully adjusted to each individual object; representative examples of plant cells and tissues have yet to be tested intensively.

Fluorescence lifetime imaging. An alternative way of discriminating fluorescence signals emitted by bound and unbound forms of the ion probe is offered by their different lifetimes (Szmacinski and Lakowicz 1995a). This fluorescence parameter, which is independent of the signal intensity, can be measured either by the timedomain method (excitation with pulsed light produced by picosecond lasers and ratioing of successively emitted signal intensities) or by the phase-modulation method. In the latter, more-widespread technique the decay of fluorescence intensity (lifetime) is represented by the phase angle and/or the modulation emitted in response to intensity-modulated light. The modulation frequency (typically in the range of 10–100 MHz) needs to be adjusted for a particular fluorescent probe. Coupled to a conventional or confocal fluorescence microscope this method yields maps of either phase or modulation data, a series of which can be used to calculate a lifetime image that mirrors local ion concentrations. Successful examples are the mapping of Ca²⁺ distribution in animal cells with the probes Quin-2 (Lakowicz et al. 1992, 1994), Calcium Green (Sanders et al. 1994) and carboxySNAFL-1 (Gerritsen et al. 1994). As lifetime images are independent of local fluorescence intensities they do not require the ion probe to display ratioable shifts of the excitation or emission spectra. Thus a broader range of ion indicators can be used, including those which allow long-wavelength excitation and hence display reduced phototoxicity and photobleaching (Lakowicz et al. 1992, 1994). The phase-modulation methods allow the simultaneous acquisition of data at all pixels of the optical plane, i.e. no pixel-for-pixel scanning is necessary. As extensive computational work is required for image acquisition and data processing the total operation time to obtain a lifetime ion map is in the range of a minute and hence limits its application to dynamic processes. Current improvements in optics, CCD cameras and computerization will considerably shorten the operation time (Szmacinski and Lakowicz 1996). A promising route to be followed in the near future is the combination of lifetime imaging (frequencyor time-domain version) with two-photon microscopy by using the advantages of pulsed NIR microbeams (König et al. 1996b; Gadella 1999).

The probes

Probes for use in ion mapping have been designed to meet the following criteria: (i) a strong shift in their fluorescence spectrum or intensity upon binding of the target ion (in order to allow a sufficient sensitivity and dynamic range of detection); (ii) high quantum yield of light emission and high photostability (in order to allow experiments at low intracellular concentrations which minimize intracellular buffering); (iii) a sufficient degree of intracellular accumulation, slow leakage out of the cell and low cytotoxicity.

Since in a distinct molecule not all desirable properties are realized to the same extent, each probe needs to be carefully selected and tested for a given cell type and experiment (cf. Hoyland 1999, to avoid known artifacts).

Table 1. Fluorescent probes for the imaging of intracellular pH

Chlorophyll-containing cells and tissues provide a specific problem due to the red fluorescence of this compound which is excited even between the maxima of around 430/450 nm and 660/640 nm (chlorophyll a/ chlorophyll b, respectively). Interference by chlorophyll fluorescence can be avoided or minimized by using probes with light emission well below 600 nm and high fluorescence yield, careful filtering of the emission light (modern detection systems allow emission spectra to be obtained at distinct cellular areas) and/or subtraction of non-probe fluorescence by digital image processing. In some cases the anatomy of the cell may allow chloroplast-free areas to be defined for confocal imaging. The lifetime of chlorophyll fluorescence shows clear differences from that of other fluorophores, making lifetime imaging an elegant way to circumvent any interferences (Gadella 1999). Aequorin-based luminescence measurements of Ca²⁺ are also not significantly influenced by chlorophyll (cf. below).

So far, only probes for imaging pH and Ca²⁺ concentrations are in routine use. Tables 1 and 2 offer a selection of the most useful probes for mapping of pH and Ca²⁺, respectively, and their binding and spectral data. For more-detailed information on ion-selective fluorescent indicators, including spectra and formulae, the reader is referred to Haugland (1996) and Haugland and Johnson (1999).

pH indicators

All the pH indicators presented in Table 1 display shifts in their fluorescence spectra upon conversion from the protonated ("acidic") to the anionic ("basic") form(s) and can thus be used for ratiometric mapping. Compared with their parent compound fluorescein the modern probes bear additional carboxyls that increase their polarity and intracellular retention. Today, the most widely applied probes for the mapping of cytosolic pH are cSNARF-1, a seminaphthorhodafluor dye that allows both excitation and emission ratioing (Cody et al. 1993; Parton et al. 1997; Yassine et al. 1997) and

Name	pK _a	Spectral optima (nm), ratioing modes ^a	
		Excitation ^b	Emission
CarboxySNAFL-1 (cSNAFL-1)	7.8	508/540 (490/540)	543/623 (540/630)
CarboxySNARF-1 (cSNARF-1)	7.5	548/576	587/635 (580/640)
SNARF calcein	7.2	552, 574	535/625
2',7'-Bis-(2-carboxyethyl)-5-(and-6-) carboxyfluorescein (BCECF)	7.0	482/503 (505/440i)	520, 528
5-(and-6-) Carboxyfluorescein (CF)	6.4	475/492 (490/450)	517
5-(and-6-) Carboxy-2',7'- dichlorofluorescein (CDCF)	4.8	488/504 (490/440i)	529
DM-NERF	5.4	497/510 (488/514)	527, 536
CL-NERF	3.8	504/514 (488/514)	540
Oregon Green	4.7	478/492 (490/440i)	518

^aRatio reads: optimum of protonated/optimum of anionic probe, in parenthesis: typical settings of filter or laser lines

^bAbsorption optima are given; these are close to excitation optima but less sensitive to the environment of the molecule (Tsien 1989; Haugland 1996)

Table 2. Probes for imaging intracellular $C_{\alpha^{2+}}$

Name	K_d (nM)	Spectral optima (nm), ratioing modes ^a	
		Excitation ^b	Emission
UV - excitation			
Fura-2	145	335/363 (340/380)	512
Bis-Fura-2	370	338/366 (340/380)	511
Mag-Fura-2	25 000	329/369 (340/380)	511
Indo-1	230	330, 346	401/475 (405/485)
Quin-2	60	333, 353	495
Excitation by visible light			
Fluo-3	390	503	526 (Ca ²⁺ -bound)
Rhod-2	570	549	581 (Ca ²⁺ -bound)
Fura Red	140	436/472 (420/480)	637, 657
Calcium Green		, , , , ,	,
-1	190	503	536
-2	550	503	536
-5N	14 000	503	536
Calcium Orange	185	549	582
-5N	20 000	549	582
Calcium Crimson	185	590	615
Oregon Green-488 BAPT	4		
-1	170	494	523
-2	580	494	523
-5N	20 000	494	523

^aOptima are given in the order Ca^{2+} -bound form, ion-free form or in the case of ratioable optima as quotient: ion-bound /ion-free probe. *Parenthesis*, typical settings of filters or laser lines

BCECF, a carboxyfluorescein derivative used for excitation ratioing (Haugland 1996). The SNAFL probes are seminaphthofluoresceins that, in contrast to cSNARF-1, display a stronger emission in their protonated than in their unprotonated form. In the moreacidic range (e.g. in vacuolar organelles), halogenated fluoresceins such as CDCF or the rhodamine-derivatives Cl-NERF, DM-NERF are suitable due to their pK_a of < 6. A new development are the LysoSensor dyes, different heterocycles with basic side chains that can be trapped in their protonated form in acidic organelles. In contrast to fluoresceins or cSNARF-1 they display increasing fluorescence intensity at decreasing pH and may thus prove useful for the ratiometric detection of low pH values. As these probes are likely to accumulate in organellar membranes, quantitative measurements require the determination of fluorescence spectra of the membrane-bound molecules (Haugland 1996).

Recently, pH-sensitive mutants of the green fluorescent protein (GFP) of Aequorea victoria have been introduced into animal cells by gene transfer and could be successfully used for pH measurements (Llopis et al. 1998). These photoproteins are now available with different pKs and display sufficient differences in either excitation or emission in the pH range between 5.5 and 8. Compartment-specific expression vectors allow the targeting of pH-reporting GFPs (fused to organellespecific proteins) to the cytosol, nucleus, the trans-Golgi compartment or the mitochondrial matrix. This approach has the potential to extend fluorescence pH-topography to intracellular sites that are "invisible" to light microscopy (i.e. not resolved by visible light transmission) but emit detectable fluorescence.

Ca²⁺ indicators

Estimates of resting levels of cytosolic free Ca²⁺ are between 100 and 200 nM; the ER and mitochondria may contain around 1 mM, cell wall and vacuolar stores 1–10 mM of Ca²⁺ (Knight et al. 1996; Trewavas and Malho 1998).

Ratiometric Ca²⁺ probes suitable for the 100-nM range require UV excitation and hence probes are desired that fluoresce sufficiently at a minimum of irradiation. Quin-2, a relative of EGTA was the prototype indicator of cellular Ca²⁺ mapping (Tsien 1980). The low fluorescence yield of this compound requires millimolar cellular concentrations to be accumulated (Chae et al. 1990) that cause substantial buffering of cellular Ca²⁺ (Ashley 1986) and inhibiting effects on growth and energy metabolism (Wolniak and Bart 1985; Gilroy et al. 1989) some of which have been attributed to formaldehyde and other products of acetoxymethylester hydrolysis (Cork 1986).

Actually, Fura-2 appears to be the most useful among the ratiometric Ca^{2^+} probes as it allows dual excitation ratioing based on a bright fluorescence. Its dimer, bis-Fura-2, has a diminished affinity and a higher dynamic range for Ca^{2^+} making it useful for the imaging of higher concentrations of this ion (around 1 μM). In the range of 1–100 μM Ca^{2^+} , ratiometric imaging is only possible with probes like Mag-Fura-2 or Mag-Indo-1, i.e. compounds that were developed as Mg^{2^+} indicators ($K_d\text{s}$ around 2 mM, i.e. close to the usual cytoplasmic Mg^{2^+} concentrations) but their affinities for Ca^{2^+} are still two orders of magnitude higher.

^bAbsorption optima are given (these are close to excitation optima but less sensitive to the environment of the molecule). (Tsien 1989; Haugland 1996)

Their use in intact cells is problematic as fluorescence shifts caused by changes in cytoplasmic Mg²⁺ have similar spectral properties and thus cannot easily be corrected.

Calcium probes excitable by visible light are mostly non-ratiometric. Most of them contain a fluorescein-derived chromophore linked to the chelator 1,2-bis(2-aminophenoxy)ethane-N,N,N',N'-tetraacetic acid (BAPTA). Indicators of the Fluo-3 type and Calcium Green-2 practically do not fluoresce in the absence of Ca²⁺ and produce a more than a 100-fold increase in emission intensity upon ion contact, which makes them well suited for the detection of small changes in cytoplasmic Ca²⁺. Calcium Green-1, on the other hand, displays a higher quantum efficiency in the free and Ca²⁺-bound state than Fluo-3 and thus allows both resting and excited cells to be vizualized at low excitation energy. Calcium shifts in the micromolar range are best detected with the low-affinity indicators Calcium Green-5N, or Calcium Orange-5N, as their fluorescence is not influenced by normal Mg²⁺concentrations and their high dissociation rates facilitate monitoring of fast spikes of Ca²⁺.

Oregon Green 488 BAPTA indicators are more efficiently excited at the 488-nm spectral line of the argon ion laser than other Ca2+ probes and should therefore be preferred for imaging by confocal laser scanning microscopy (Haugland 1996). Calcium Green-1 is the only visible-light excitable probe useful for fluorescence lifetime imaging (Lakowicz et al. 1994; Sanders et al. 1994; Haugland 1996). Also some ratiometric Ca²⁺ probes exhibit advantages when used in lifetime measurements. The apparent calcium dissociation constant of Fura-2 calculated from phase angle or modulation data changes strongly with the excitation wavelength (Szmacinski and Lakowicz 1995b). This might open the possibility of simultaneously detecting low and high calcium concentrations by using two bands of excitation (e.g. 345 nm for [Ca²⁺] around 50 nM and 380 nm for $[Ca^{2+}]$ around 20 μ M). Indo-1, which is commonly in use as an emission ratiometric probe, can likewise be used for the lifetime imaging of Ca²⁺ at its 475-nm emmission band; furthermore, two-photon excitation at 702 nm instead of UV excitation can be applied (Szmacinski et al. 1993).

Aequorin-luminescence: an alternative to fluorescence-based Ca^{2+} imaging

Aequorin is a Ca^{2^+} -sensitive photoprotein complex of some coelenterates and consists of the 22-kDa protein apoaequorin, the luminophore coelenterazine (MW 432) and molecular oxygen. Upon binding of three Ca^{2^+} to this complex coelenterazine is oxidized to coelenteramide and blue luminescent light is emitted. The measurement of Ca^{2^+} with aequorin exploits the high sensitivity of its luminescence intensity to the Ca^{2^+} concentration and its wide dynamic range (0.1 to > 100 μ M) which is unparalleled by fluorimetric Ca^{2^+} assays. As no illumination is needed, complications

caused by autofluorescence, phototoxicity and bleaching are avoided. Unfortunately, a broad use of externally added aequorin is limited by the relatively complicated loading of the apoprotein into cells, a process which requires either electroporation (Gilroy et al. 1989), microinjection (large algal cells: Tazawa et al. 1995; Okazaki et al. 1996) or other invasive techniques (see Miller et al. 1994 for a review). Nevertheless, in carrot or barley protoplasts loaded by electropermeabilization, aequorin, in contrast to Quin-2, caused less or no derangement of ATP metabolism and did not inhibit cell division (Gilroy et al. 1989). In recent years, the genetic transformation of plant cells with an apoaequorin gene (located on commercially available expression vectors) opened a way to express sufficient apoaequorin in the plant cells to be examined (see Knight and Knight 1995 for a review). After transient or constitutive expression of the apoprotein the functional aequorin is reconstituted by incubating the transgenic plant tissue for 4-6 h with the membrane-permeant coelenterazine. Different synthetic coelenterazine analogs are available that endow the resultant aequorin (then termed "semisynthetic") with different Ca²⁺ affinities or with spectral properties that allow quantification of Ca²⁺ by twowavelength ratioing (Shimomura et al. 1988; Shimomura 1991) and simplify its calibration (Knight et al. 1993). The Ca²⁺ measurements with transgenic aequorin were first performed with the apoprotein present in the cytosol and by simple luminometry of whole seedlings, leaves, roots or suspensions of cultured cells. This approach proved successful in the quantification of changes in cytoplasmic calcium levels in response to a variety of external stimuli including touch, cold shock, elicitors (Knight et al. 1991, 1992, 1993; Chandra and Low 1997), hydrogen peroxide (Price et al. 1994), and anoxia (Sedbrook et al. 1996). Microscopic imaging of Ca²⁺ distribution in aequorin-expressing plants has been done on whole cotyledons, hypocotyls and roots (Knight et al. 1993). However, due to the insufficient luminescence intensities of individual plant cells the transgenic approach has not yet reached the cellular or subcellular level of Ca²⁺ mapping. This limitation can partially be compensated for by the option of targeting the apoprotein to distinct intracellular sites and reporting changes in Ca²⁺ close to such microdomains. By means of apoaequorin expression vectors with appropriate targeting sequences that work in plant cells the photoprotein has been directed to chloroplasts (Johnson et al. 1995), ER and to the cytoplasmic side of the vacuolar membrane (Knight et al. 1996). In the latter case a fusion protein of apoaequorin with the vacuolar pyrophosphatase was expressed and reported a coldinduced release of Ca²⁺ from the vacuolar pool. In animal cells, apoaequorin was successfully targeted to the nucleus (Brini et al. 1994), mitochondria (Rizzuto et al. 1993) and ER (Kendall et al. 1994). Engineered aequorins should soon become available that combine different colors of emission light with specific targeting sequences and therefore allow the simultaneous visualization of Ca²⁺ concentrations at different subcellular locations.

Actual limitations of the aequorin methods are the specific efforts and risks of transformation protocols, sometimes insufficient rates of expression of transgenes (Sedbrook et al. 1996) and interference from changing cellular Mg²⁺ concentrations (Trewavas and Malho1998).

Calmodulin-based Ca²⁺ probes

The latest approach to Ca2+ imaging is offered by the chamaeleon dyes, i.e. calmodulin molecules that are substituted at their flanking regions with mutants of GFP, typically a blue-emitting GFP at the one side and a yellow-emitting one at the other. After expression in the target cell, binding of Ca²⁺ to the calmoduline moiety results in a conformational shift that shortens the distance between the GFPs thus allowing increasing transfer of fluorescence resonance energy from the blueemitting donor-GFP to the acceptor-GFP. This process is best quantified by ratioing the emission intensity of acceptor- and donor-GFP (Miyawaki et al. 1997). Experiences with chamaeleon probes expressed in plant cells should soon be available. The possibility of confocal ratio imaging of their fluorescence emission might open promising developments for Ca²⁺ imaging in transformed cells and should provide motivation to apply the principle of fluorescent protein hybrids to the mapping of other small signal molecules.

Probes for the mapping of other ions

Though not yet reported, imaging of magnesium is now within the reach of fluorescence microscopy. The excitation-ratioable compounds Mag-Fura-2, Mag-Fura-5 and Mag-Indo-1 appear most promising for such purposes. These compounds have already been referred to as lowaffinity Ca²⁺ probes and can be used with optical equipment and procedures similar to those established for Ca²⁺. Comparing their affinities for Mg²⁺ and Ca²⁺ (cf. above) indicates that fluorescence shifts due to the binding of free cytoplasmic Mg²⁺ (e.g. around 0.5 mM in Vigna mungo root tips, Yazaki et al. 1988) are not influenced by cytoplasmic Ca²⁺ concentrations ≤1-2 µM. Fluorescence lifetime imaging can be done wih the probes Magnesium Green and Magnesium Orange for low Mg²⁺ concentrations and with Mag-Quin-2 for higher concentrations (Szmacinsky and Lakowicz 1996).

Ratio imaging of potassium can be done with the crown ether compound benzofuranyl isophthalate (PBFI). This probe is only 1.5-fold more sensitive to K⁺ than to Na⁺ but cellular K⁺ is usually present at a more than 10-fold higher concentration. The cell impermeant tetraammonium salt of PBFI is applicable for imaging K⁺ efflux or apoplastic K⁺, as demonstrated at leaves of *Vicia faba* (Muhling and Sattelmacher 1997).

Imaging of sodium in the range from 0.5–50 mM appears now feasible with the benzofuranyl crown ether probes SBFI and SBFO, which have K_ds in the 10–100 mM range that are strongly shifted by physio-

logical K^+ concentrations. The new visible-light excitable probe Sodium Green, a fluorescein-linked crown ether, shows an improved (41-fold) selectivity for Na^+ over K^+ (Haugland 1996). This probe is also useful for lifetime measurements: though discrimination of Na^+ against K^+ is only 11- to 15-fold with respect to K_d , the magnitudes of changes in phase angle or modulation due to K^+ binding are much lower compared to Na^+ (Szmacinsky and Lakowicz 1997).

Many of the above-mentioned non-ratiometric indicators for Ca²⁺ and Mg²⁺ exhibit high fluorescence intensities when bound to heavy-metal cations (Kuhn et al. 1995; Haugland 1996). Even though specific respones to some metal cations (e.g. those of Calcium Green to Tb³⁺, Cd²⁺, Hg²⁺ and Ni²⁺) are much stronger than that shown with Ca²⁺ or Mg²⁺ the abundance of the latter cations naturally hampers quantification and imaging of heavy metals by competition for the probe. Nevertheless, under conditions where significant changes in the Ca²⁺ and Mg²⁺ concentration(s) can be excluded and additional data are available to identify the ion responsible for the measured fluorescence shifts, imaging of heavy metals appears manageable: in animal cells (pituitary gland and glial) loaded with Fura-2 the uptake and distribution of Cd²⁺ could be followed by excitation ratio imaging (Hinkle et al. 1992). The correlation of the observed signals to the Cd²⁺ concentration was supported by the effect of tetrakis-(2-pyridylmethyl)ethylenediamine, a membrane-permeant chelator with extremely high affinity for heavy metals, that reversed the increase in the fluorescence ratio.

Some heavy-metal cations, notably Mn^{2+} , strongly quench the fluorescence of Ca^{2+} indicators at all excitation wavelengths, including the isosbestic point. This effect occurs only with the fully de-esterified probe and can be exploited to improve Ca²⁺ imaging, e.g. by correcting or reducing fluorescence of extracellular probes, or to calibrate their spectral responses (Indo-1 and Fluo-3: Gilroy and Jones 1992). Furthermore, as Mn²⁺ is a high-affinity transportant of several Ca²⁺permeable channels (Piñeros and Tester 1995), the fluorescence quench of an intracellular Ca²⁺ probe measured at its isosbestic (Ca²⁺-insensitive) wavelength, which occurs after adding external Mn²⁺, can be used to monitor the uptake of this cation and hence the activity of Ca²⁺ channels (McAinsh et al. 1995; Grabov and Blatt 1998b). Similiarly, quenching of Fura fluorescence in excited Chara cells that were pre-incubated with Mn²⁺ suggests a release of pre-accumulated Mn²⁺ (thought to substitute for Ca²⁺) from internal stores (Plieth et al. 1998).

Procedures, problems and solutions

Loading of fluorescent ion probes

Ion imaging requires a sufficient concentration of the ion-sensitive form of the probe to be present in the cell or the subcellular area of interest. Most ion probes are polar and membrane impermeant in the physiological

range of pH. Several strategies have been invented that aim at the accumulation of these molecules and their maintenance in the target cell.

Permeant esters. Many fluorescent ion probes that bear hydroxyl or carboxyl groups are available as acetyl- or acetoxymethyl (AM) esters, respectively. These lipophilic molecules are designed to penetrate cellular membranes, to be cleaved by cellular esterases and the anions formed to be trapped inside the cell. This principle opens the simplest and least invasive way of accumulating the desired probe and works with many plant cells and tissues. Examples comprise coleoptiles and hypocotyls (Gehring et al. 1990a,b, 1994), mesophyll cell protoplasts (Giglioli-Guivarc'h et al. 1996), root epidermal cells (Brauer et al. 1996), pollen tubes (Fricker et al. 1994b), algae (Berger and Brownlee 1993) and cultured plant cells (Roos 1992; Roos et al. 1998; Fig. 1). Mature plant tissues are often found to give insufficient loading with AM esters (Gilroy et al. 1991; Hodick et al. 1991) and thus require alternate loading strategies. One reason may be the presence of cell-wall-bound esterases that cleave the esters before they cross the plasma membrane (Cork 1986). In such cases, advantage can be taken of the different temperature dependences of membrane transport and chemical cleavage of AM esters: as an example, incubation of wheat root cells at low temperature (4 °C, 2 h) allowed sufficient accumulation of Fluo-3 AM which was then cleaved intracellularly by raising the temperature to 20 °C (Zhang et al. 1998). Increasing the solubility of AM esters in the incubating solution by the mild disperging agent pluronic acid F-127 may also increase the loading efficiency without impairing cell integrity (Granados et al. 1997).

Alternative loading strategies. Cells may be loaded by incubating them with the indicator free-acid at a low external pH. Ion probes with carboxylic or phenolic groups are protonated at an acidic external pH and the lipophilic acids can penetrate the plasmalemma followed by trapping of the anions formed at the near-neutral pH of the cytosol. This method is preferentially applicable to cells that usually exist in or are not stressed by an acidic environment. Successful 'acid loading' has been reported with Indo-1 in plant protoplasts and algal cells (Lynch et al. 1989; Russ et al. 1991), root hairs (Wymer et al. 1997) and with cSNARF-1 in fungal hyphae (Bachewich and Heath 1997). Problems arising from the ion-exchange properties of the plant cell wall could be reduced by masking charges with high salt concentrations (Hodick et al. 1991).

Cutinase treatment together with low-pH incubation allows the cutin barrier of intact leaves of *Lemna gibba* to be overcome and Fluo-3 or BCECF to be loaded into the cytoplasm (Fricker et al. 1994b). This may be an alternative to removing the cuticule by scraping or tape adhesion. The loading of AM esters is not applicable together with cutinase treatment as even traces of this enzyme hydrolyse the dye esters outside the cell.

Microinjection allows loading of a variety of ion indicators into the cytoplasm of individual, large cells

that are impaled by a micropipette. These techniques are all invasive and must therefore include tests to ensure that the cell under study is not severely compromised; nevertheless, wound reactions and unwanted dilution of the cytoplasm by the pipette solution have to be taken into account. Pressure injection has been used for the introduction of Fura-2-dextran into pollen tubes of Papaver (Franklin-Tong et al. 1997) and of Calcium Green dextran into papillae of *Brassica* (Dearnaley et al. 1997). Iontophoretic loading forces dye bulk flow into the cell by a constant or pulsed current of typically 1–5 nA, and has been used successfully with guard cells of Commelina communis and Vicia faba (Fluo-3, Indo-1, BCECF or Fura-red: Fricker et al. 1994a; Fura-2 and BCECF: Grabov and Blatt 1997) and root hair cells of alfalfa (Calcium Green-dextran and Fura-2-dextran, Ehrhardt et al. 1996). Loading through a patch microelectrode has been used in animal cells to combine recordings of whole-cell currents and the perfusion of the cellular interior with the fluoroprobe contained in the electrode (cf. Neher and Augustine 1992).

The microinjection of ion indicators entrapped in liposomes appears to open a way to the ion mapping of

Figs. 1–3. Accumulation of pH-probes and pH-imaging exemplified in cultured cells of *Eschscholzia californica*. Some cytoplasmic/nuclear regions and vacuoles are indicated by c/n or v, respectively

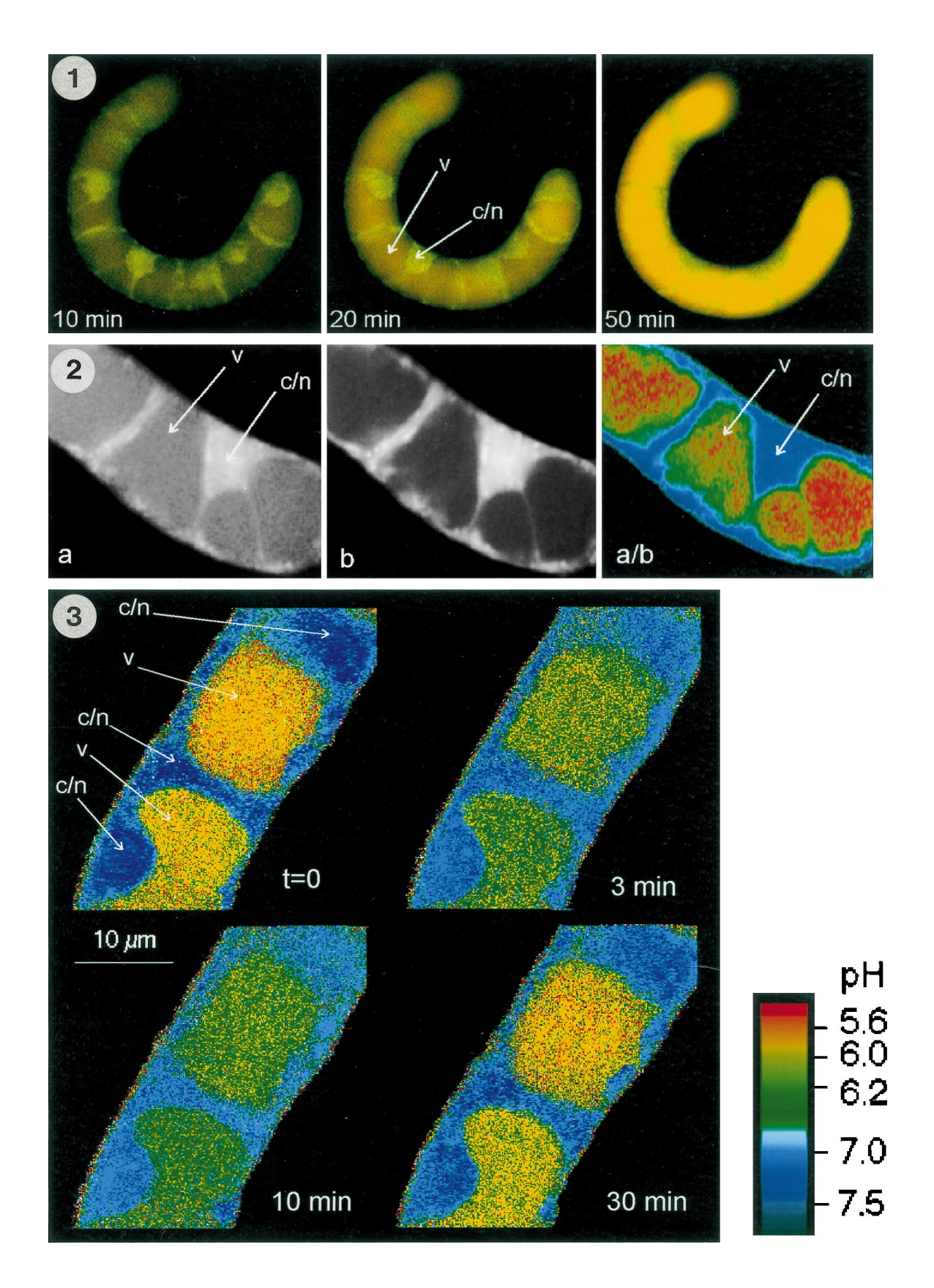
Fig. 1. Ester loading of 5-carboxyfluorescein. Cells were incubated with a 5 μ M solution 5-carboxyfluorescein diacetate acetoxyymethyl ester (CFDA-AM) in culture liquid. At the times indicated, conventional fluorescence images were obtained with a Nikon Diaphot microscope (λ Ex = 440, λ Em > 520 nm) and digitised with a Sony 3CCD camera. The fluorophore first accumulates in the cytoplasmic/nuclear region and is then transferred to the vacuole

Fig. 2. Loading of and confocal pH mapping with cSNARF-1. After 60 min of incubation with 5 μM cSNARF-1-AM in culture liquid, fluorescent CLSM images were acquired using a Leica confocal microscope. Excitation: argon ion laser at 514 nm. Two images were scanned simultaneously at the following emission wavelengths: channel $1 = 583 \pm 5$ nm (a), channel 2 = >610 nm (b). Panels a and **b** represent mainly the acidic and the anionic form of the probe, respectively. Autofluorescence was eliminated by appropriate settings of the photomultiplier detectors. a/b Intensity ratio of channel 1/ channel 2 for each pixel. The ratios are color coded according to the pH scale shown below. In this scale, intensity ratios were related to pH by means of a calibration graph obtained with cells that had accumulated the probe and were then suspended in Mes buffers of different pH. They contained the detergent cetyltrimethylammonium bromide which caused a rapid equilibration of fluorescence between most parts of the cells and the outer medium. Similar calibration graphs were obtained with the fluorescence emitted from cytoplasmic/ nuclear or vacuolar areas by the nigericin/KCl method in the presence of methylamine or butyric acid (cf. text and Roos et al. 1998). The pH map (a/b) mainly reports the typical pH gradient between the cytoplasmic/nuclear area (pH near 7.4) and the vacuoles (between 5.6 and 6.1)

Fig. 3. Confocal pH topography with cSNARF-1 in elicitor-treated cells. The pH maps were obtained as described in Fig. 2. Cells were fixed on agar in a perfusion chamber and at t=0 received 1 μ g/ml of an elicitor preparation of baker's yeast. Confocal fluorescence images were scanned at the times indicated. The maps report a transient decrease in the vacuolar pH in parallel with an acidification of the cytoplasmic/nuclear region (taken from Roos et al. 1998)

endo- or exocytotic compartments: liposomes of 70 nm diameter containing BCECF or similar probes were injected into human skin fibroblasts together with ATP and delivered their fluid-phase contents selectively into

the trans-Golgi compartment as assessed by co-localization with the trans-Golgi stain C-6-NBD-ceramide. This procedure allowed for the first time the confocal ratio imaging of trans-Golgi pH (Seksek et al. 1995).



Intracellular distribution of fluorescent ion probes

Once accumulated, ion probes may undergo intracellular redistribution or even extrusion. Knowledge of these processes is a prerequiste for obtaining and correctly interpreting ion maps. Some of these aspects have been detailed in earlier reviews (Fricker et al. 1993; Williams et al. 1993).

The initial distribution of ion probes liberated from internalized esters reflects the compartmentation of the involved esterases. Substantial species differences exist in this respect. Data from maize root hair cells indicate that different, dve-selective AM esterases are active in the cytoplasm and in the vacuole: incubation with BCECF-AM led to the exclusive accumulation of fluorescence in the vacuole (Brauer et al. 1995, 1996, 1997) whereas BCECF acid that had been loaded via low-pH incubation or microinjection was retained almost exclusively in the cytoplasm (Brauer et al. 1996). In contrast, fluorescence liberated from cSNAFL1-AM was confined to the cytoplasm. Esterase activities measured in crude cell extracts displayed a pH optimum of about 5.0 for BCECF-AM and about 7.0 for cSNAFL1-AM. Thus, esterases specific for BCECF or cSNAFL-1 are likely to be present either in the vacuole or the cytoplasm, respectively (Brauer et al. 1996).

In other cells, BCECF-AM, at least at low concentrations, seems to be split in the cytoplasm (protoplasts of *Digitaria*: Giglioli–Guivarc'h et al. 1996) followed by the transfer of the fluorophore into vacuolar or other vesicles (protoplasts of *Arabidopsis* and pollen tubes of *Lilium longiflorum*, Fricker et al. 1994b).

Experiments with CFDA-AM (carboxyfluorescein bearing one acetoxymethylated carboxyl and two acetylated hydroxyl groups) suggest the lack of an active AM esterase in a plant vacuole: in cultured cells of *Eschscholzia*, all esterified groups are readily split off in the cytoplasm as seen by the rapid accumulation of cytoplasmic fluorescence followed by the transfer of the fluorescent, i.e. de-esterified compound, to the vacuole (Fig. 1). After selective permeabilization of the plasma membrane by osmotic treatment the vacuoles do not accumulate any fluorescence during perfusion with the same AM ester but are able to liberate and accumulate carboxyfluorescein from the diacetate (data not shown).

Similiarly, cSNARF-1-AM, which bears one acetoxymethyl and one acetyl group, is completely deesterified in the cytoplasm and the fluorescent molecule transferred to the vacuole. The extent of this transfer differs among species: in most plant cells sufficient fluorescence remains in the cytoplasm for over 1 h or longer, e.g. cultured cells of *Gossypium* (Roos 1992) and of *Eschscholzia* (Roos et al. 1998; Fig. 2) and *Zea* root cells (Brauer et al. 1996), whereas rapid vacuolar sequestration has been observed in *Neurospora* hyphae, *Agapanthus* pollen tubes and *Dryopteris* rhizoids (Parton et al. 1997).

Generally, it appears that probes requiring a high number of ester groups to be cleaved (e.g. five in BCECF, five in most calcium indicators, four in SNARF-calcein) show a strong tendency to become sequestered in the vacuole or in related vesicles, whereas probes with a lower number of ester bonds (e.g. cSNARF-1 with one esterified carboxyl and one esterified hydroxyl) tend to be retained longer in the cytosol and to yield brighter fluorescence (Roos 1992; Fricker et al. 1993; Slayman et al. 1994; Roos et al. 1998). This argues that the specificity and/or activity of cytoplasmic esterases limits the degree of cleavage of internalized esters.

Fluorescence observed in the cytoplasmic area by conventional fluorescence microscopy may not only originate from indicator molecules dissolved in the cytosol but also from those entrapped within endomembranal vesicles. Generally, a high organellar density can obscure the location of "cytoplasmic" fluorescence shifts. As an example, in coleoptile tips the distribution of Fluo-3 appeared relatively "even" throughout the cytoplasm when examined by conventional epifluorescent illumination, whereas subsequent confocal laser scanning microscopy of the same cells revealed "punctuate" fluorescence, i.e. localization in vesicular structures (Williams et al. 1993). Similar patterns of distribution were found with non-esterified probes loaded via microinjection (Fricker et al. 1994b). It appears, therefore, that in less-vacuolated plant cells (e.g. pollen tubes or coleoptiles, but not guard cells) the free-acid forms of ion probes tend to become sequestered into the endoplasmic reticulum, mitochondria and other small vesicles.

Vesicular compartmentation dominates the distribution of highly esterified probes in fungal hyphae: in Neurospora crassa, BCECF or SNARF-calcein (a derivative of cSNARF-1 containing two additional iminodiacetic ester groups) liberated from its AM esters accumulated both in the vacuolar network and in endomembranal vesicles of different size; the smallest of them might even escape the resolution of the light microscope (Slayman et al. 1994). Calcium Green, Fura-2 and Indo-1 became highly sequestered in vacuolar or reticular vesicles of three taxonomically unrelated fungal species irrespective of whether the hyphae were incubated with AM esters or microinjected with 10-kDadextran conjugates of these dyes (Knight et al. 1993). In this context it should be realized that AM esters of ion probes tend to form micelles in buffers of physiological ion concentrations, a process which might favour their uptake and cellular transfer via endocytotic vesicles. As vesicle traffic is more temperature dependent than diffusional transport, incubation with AM esters at low temperature might reduce vesicular sequestration of ion probes (Shorte and Bolsover 1999). Summarizing, for an exact localization of fluoroprobes - and hence the iondependent processes to be measured – confocal fluorescence scanning microscopy is often indispensable. If a "cytoplasmic" location is assumed, the experimenter should clarify whether the fluorescence emission used for imaging can really be attributed to the cytosolic phase (which may still include submicroscopic vesicles) or rather represents an average of all extravacuolar organelles.

The mechanisms behind the intracellular traffic or the efflux of accumulated ion probes have not yet been investigated systematically. While many data support the non-facilitated diffusion of lipophilic species (e.g. the correlation of retention time and polarity of fluoresceinderivatives), and the anion carrier inhibitor probenicid did not influence the sequestration of Calcium Green, Fura-2 and Indo-1 (Knight et al. 1993), active transport steps cannot yet be excluded. Data from insect cells indicate the extrusion of the AM esters (not of the free acids) of the Ca²⁺ indicators Fura-2, Quin-2, Indo-1, Fluo-3, Calcein and of the pH probe BCECF via multidrug-resistance (MDR) transporters of the p-glycoprotein type (Homolya et al. 1993; Brezden et al. 1994). From bacterial cells, BCECF is extruded via an ATP-driven extrusion system for organic anions (Glaasker et al. 1996). The MDR transporters are members of the ABC superfamily that catalyse MgATP-energized, proton-motive-force-independent transport of organic solutes and exist also in plant cells (Dudler and Hertig 1992). Another subclass of the ABC family, the multidrug-resistance-associated proteins (MRP) comprises the well-known GS-X pumps of the plant vacuolar membrane, which not only transport glutathione-S-conjugated xenobiotics but also some amphipathic organic anions (Rea et al. 1998). In addition, other directly energized tonoplast pumps have been functionally characterized that allow, for example, the specific vacuolar uptake of sulfonated or sulfated compounds including LuciferYellow CH (Klein et al. 1997) or of glucuronides (Klein et al. 1998). Though transport of H⁺ or Ca²⁺ probes by any vacuolar transporter has not yet been demonstrated there is clearly a need for investigations on plant vacuolar transport of fluorescent ion probes.

Macromolecular conjugates of ion probes

Dextran conjugates. An effective way to prolong the retention time of ion probes in the cytosol is by their conjugation to macromolecules. Dextran conjugates (MW between 10 kDa and 1000 kDa) of most of the actual pH, Ca²⁺ and Na⁺ probes are available. These can be loaded into cells by microinjection or by incorporation into liposomes that are then fused to protoplasts. Microinjected dextran conjugates are usually well retained in the cytoplasm of plant cells and are less likely to be sequestered into the vacuolar system than probes liberated from AM esters. For example, dextran conjugates of Calcium Green and of cSNARF-1 remained in the cytoplasm of Fucus zygotes (Berger and Brownlee 1993), of Neurospora hyphae and Agapanthus pollen tubes (Parton et al. 1997). By contrast, injected dextran (10 kDa) conjugates of Calcium Green-1, Fura-2 or Indo-1 did not escape the high endocytotic activity of fungal cells and became sequestered in the hyphal vacuolar network of Basidiobolus, Neurospora and *Uromyces* much like their unconjugated analogues (Knight et al. 1993).

Covalent coupling of ion indicators to cellular constituents. Some ion indicators, mostly pH probes, can be loaded as reactive molecules that allow their conjugation

to cellular constituents. The membrane-permeant compounds chloromethylfluorescein diacetate (CMFDA) and chloromethylSNARF-1 acetate react with cellular glutathione (catalyzed by glutathione-S-transferase) and with cysteine-containing proteins; the adducts formed show substantially longer retention times compared with the non-reactive molecules. The chloromethyl derivatives are non-fluorescent until the above conjugates are formed and the acetates are split off. Many glutathione-S-conjugates are transported into plant vacuoles by ATP-dependent pumps (e.g. Tommasini et al. 1993; Coleman et al. 1997; Rea et al. 1998). Expectedly, after incubation of epidermal cells of *Hordeum vulgare* with CMFDA, the fluorescence originally accumulated in the cytosol moved slowly into the vacuole (Fricker et al. 1994b). Another approach to conjugate ion probes to intracellular macromolecules involves amine-reactive dyes such as the succinimidyl ester of 5-(and 6-)carboxyfluorescein which after application to bacteria allowed continuous measurement of intracellular pH (Riondet et al. 1997).

Doubts are justified as to whether the conjugation of essential SH- or amino groups of proteins and other biomolecules causes no significant metabolic derangements and a careful analysis of the potential toxicity seems indispensable. A more promising option appears to be the use of commercially available amine-reactive derivatives for the preparation of defined dye conjugates (Haugland 1996) in order to optimize loading and the intracellular behaviour of the cell type under study.

Interaction of ion probes with cellular ions and metabolism

Ion-mapping experiments should generally be conducted at the lowest concentration of the intracellular ion probe that yields an acceptable signal-to-noise ratio in order to minimize potential impairments of cellular functions. A good compromize must take into account the fluorescence properties of the probe (e.g. quantum yield, dynamic range, bleaching), its distribution in the cell of study (rate of accumulation, compartmentation, quenching, relation to background fluorescence), initial ion concentrations as well as altitude and rapidity of the expected shifts and, last but not least, the sensitivity and accuracy of the available detection system(s).

A few estimates of sufficient intracellular probe concentrations have been provided by comparing local fluorescence intensities in loaded cells with those of standard preparations of the active probe in known cell-sized volumes as liquid droplets in oil emulsions (Gilroy et al. 1991) or defined volumes (voxels) of confocal images. They range from 5 to 20 μM for Indo-1 and Fluo-3 in aleurone protoplasts (Gilroy and Jones 1992), $10\text{--}30~\mu M$ for cSNARF1 in cultured plant cells (Roos, unpublished) and around 50 μM for BCECF in guard cells (Fricker et al. 1993).

It must be realized that each ion indicator inevitably adds to the cellular buffering capacity for the ion of interest and thus influences its local concentration. In

the case of pH probes such deviations might appear negligible if the above estimates for cSNARF1 and BCECF are compared with the high H⁺-buffering capacity of the plant cytoplasm: relevant figures (in mM H⁺ per pH unit at pH 7.5) range from extreme values of 90 in *Vicia* guard cells (Grabov and Blatt 1997) to the more common levels of 20-50 in root hairs of Sinapis (Felle 1987), 17.9 in Chara (Reid et al. 1989) and 14.9 in *Asparagus* mesophyll cells (Crawford et al. 1994). Analogous data for the average Ca²⁺-buffering capacity of plant cells are not available. Injection of up to 100 μM of BAPTA chelators into Fucus zygotes caused no changes in the typical Ca²⁺ gradient (Speksnijder et al. 1989), which is often quoted as an indication of a robust Ca2+ homeostasis in non-excited cells. Indeed, there is little doubt that probes like Fura-2, Indo-1 or Calcium Green do not compromise the principal Ca²⁺ distribution in plant cells and thus can be used to visualize strong shifts of cytoplasmic free Ca²⁺ (validated, for example, by observing the expected effects of Ca²⁺ ionophores or external EGTA). However, the steepness and kinetics of Ca²⁺ gradients are likely influenced by the intracellular indicators: in animal (chromaffin) cells a transient influx of Ca²⁺ was evoked by depolarizing the plasma membrane with a patch pipette and imaged with Fura-2. Almost all of the incoming Ca²⁺ was normally bound to an immobile endogenous buffer of low affinity. Increasing concentrations of Fura-2 attenuated the Ca2+ peaks and slowed the recovery time. From a well-fitting model describing fast competition between the dye and the endogenous buffer it was deduced that for the accurate imaging of Ca²⁺ peaks of 150 nM height (i.e. twice its resting concentration) Fura-2 concentrations should not be higher than 4 µM, which requires high detector sensitivity. Conversely, high concentrations of the probe (400 μM) bind virtually all free Ca²⁺ and are thus appropriate if Ca²⁺ influx rather than its intracellular distribution is to be visualized (Neher and Augustine 1992).

Intoxifications caused by modern ion probes have rarely been reported for plant cells. In animal cells (seminal vesicles) Quin-2, Fura-2 and Indo-1 were found to be oxidized by the hydroperoxidase activity of prostaglandin H synthase and thus might influence arachidonate metabolism (Van der Zee et al. 1989).

Calibration: linking fluorescence signals to ion concentrations

The relationship of fluorescence ratio or intensity to the actual ion concentration needs to be calibrated from a series of data obtained at known ion concentrations. Calibration experiments should be preferentially performed in situ, i.e. with the probe present intracellularly, in order to take into account all factors that might influence binding equilibrium and fluorescence properties in the cell or organelle of interest (ionic and macromolecular composition, viscosity, degree of deesterification, binding to cell components, quenching

etc). As an example, for the probes Fluo-3, Fura-2 and Indo-1 (Ca^{2+}), Mag-fura-2 (Mg^{2+}) and SBFI (Na^{+}) the estimates of K_d in different animal cells were considerably higher than those determined in buffered solutions (Haugland and Johnson 1999). Deviations of ion sensitivity between the external and the internalized probe are best detected if fluorescence spectra of free and esterified probes are compared between solution and cell suspensions (Owen et al. 1995). In-situ calibrations make use of an ionophore to equilibrate the intracellular to the extracellular ion concentration the latter being controlled by appropriate buffers. For some ratio dyes in-vitro calibrations performed in buffers that mimick some important components of the cell have been shown to give useful estimates of the behaviour of the indicator in vivo, at least of its dynamic range.

Mapping of Ca²⁺ is usually calibrated in-situ with the ionophores ionomycin, A-23187 or its non-fluorescent 4-bromo analogue, and external Ca²⁺-EGTA buffers. For the reasons explained earlier, accurate calibration is more complicated with single-wavelength dyes than with ratiometric indicators.

Calibration of pH mapping is often more complicated as the mechanisms governing intracellular pH homeostasis complicate equilibration of proton concentrations with the outer medium. An established in situ calibration procedure rests on the equilibration of intracellular and external pH (pH_{in} and pH_{ext}, respectively) with nigericin (an ionophore facilitating the exchange of K⁺ for H⁺) in the presence of 100-150 mM KCl (e.g. Thomas et al. 1979). Equally high K + concentrations on both sides of the plasma membrane depolarize the membrane potential and eliminate the effects of a strong transmembrane K⁺ gradient on ΔpH. In practice, besides some toxic effects of nigericin, systematic errors of about 0.2 units of the steady-state pH_{in} have been observed after such treatments, indicating slow or incomplete equilibration of cytoplasmic and extracellular pH (James-Kracke 1992; Boyarsky et al. 1996a).

A more-elegant calibration procedure has been proposed by James-Kracke (1992). Cells loaded with BCECF were titrated in the presence of the protonophores Carbonyl cyanide *m*-chlorophenylhydrozone (CCCP) or carbonyl cyanide p-(trifluoromethoxy)phenylhydrozone (FCCP) with HCl and than back with KOH in order to drive pH_{in} to values that allow the determination of minimum and maximum fluorescence ratios, which represent the fully protonated or fully deprotonated form of the intracellular indicator. By introducing these values in the Henderson-Hasselbalch equation, together with the increments of fluorescence measured over the used pH range, calibration graphs were obtained that were fairly coincident with those of the null method (cf. below). This approach requires neither complete depolarization of the membrane potential nor equilibration of proton concentrations across the plasma membrane, and hence should be applicable to a broad spectrum of cell types including plant cells (Fricker et al. 1997). It requires, however, that the dissociation constant of the intracellular probe is known, which is not generally the case in plant cells.

An alternate approach uses membrane-permeant weak acids or bases to facilitate pH equilibration. In animal cells, the so-called null method was successful in determining absolute values of pH_{in} by exposing cells to buffered mixtures of membrane-permeant acid (e.g. butyrate) plus base (e.g. trimethylamine) in concentrations that were previously determined to cause an equal deflection of intracellular fluorescence quotients in the acidic and the basic direction. Hence, no ("null") resultant effect of the mixture on pH_{in} is observed if a null solution is found whose nominal pH matches $pH_{\rm in}$. Using several null solutions the pHin as well as the cellular buffering power could be bracketed with high accuracy (Boyarsky et al. 1996a). In intact plant cells, complete equilibration of cytoplasmic and external pH under the influence of permeant acids or bases is often prevented by the high cytoplasmic buffering capacities and the pH control exerted by the vacuole. In cultured cells of *Eschscholzia* treated with permeant acids (butyric or pivalic) fluorescence ratios of cSNARF-1 responded to changes in pH_{ext} with the same slope as did the external fluorescence ratio. However, the absolute values of cytoplasmic and external fluorescence ratios remained different and coincided only after combined administration of permeant acids, nigericin and 100 mM KCl (Roos et al. 1998). In contrast, the vacuolar pH can easily be clamped to the pH of external buffers if membrane-permeant ammonia or methylamine is present, which indicates that the vacuole functions as a base trap. This has been demonstrated with BCECF in vacuoles of maize root cells (Brauer et al. 1997) and with cSNARF-1 in vacuoles of Eschscholzia cells (Roos et al. 1998).

In-situ calibration procedures generally face the problem that the identity of cellular and external ion concentrations after "equilibration" is hard to prove and hence deviations between nominated and true ion concentrations cannot totally be excluded. Therefore, comparisons are helpful between different probes and equilibration procedures as well as between the increments of intracellular and extracellular fluorescence in response to the applied ion concentration. Fortunately, with some pH probes the in-situ approach indicated a similar pH-dependence of fluorescence as the extracellular dye assayed in vitro. Calibration of BCECF in appropriate buffers (with no cells present) compared to the above null method exercised with cultured rabbit aorta cells revealed only small differences (<0.1 pH unit) that were independent of pH_{in} (Boyarsky et al. 1996b). The pH-sensitivity of cSNARF-1 measured in cultured cells of Eschscholzia did not significantly differ irrespective of whether the fluorescence quotients were measured in the vacuole (after equilibration with methylamine), in the cytosol (after equilibration with butyrate plus nigericin and KCl, cf. above), or in the external, buffered media of detergent-treated cell suspensions (Roos et al. 1998). This seemed to be in contrast with reported changes in the pK_a of cSNARF-1 inside cells (Owen 1992) that were attributed to the binding of the probe to cellular proteins (Seksek et al. 1991). However, more-recent data revealed that a

contaminant of the commercially distributed substance but not the molecule liberated from cSNARF-1 AM is able to bind to proteins (Yassine et al. 1997).

A detailed description of calibration procedures in plant cells, including aequorin-based luminescence assays of Ca²⁺, is given by Fricker et al. (1999).

Summarizing, the calibration of fluorescence data to absolute cellular Ca^{2+} or H^+ concentrations may not always guarantee a perfect match. However, in most experiments the correct monitoring of experimental *changes* in ion concentrations (ΔpH , $\Delta [Ca^{2+}]$) is of higher importance than the determination of absolute concentrations. Most experimental conditions known to affect the relation of ion concentration and fluorescence emission shift the fluorescence-versus-concentration curve in parallel rather than changing its slope. Hence, changes in ion concentrations can often be correctly mirrored even if the absolute data contain some degree of uncertainty or error (e.g. Brauer et al. 1997; Fricker et al. 1997, 1999; Parton et al. 1997; Roos et al. 1998).

Applications of Ca²⁺ and pH imaging in plant signal transduction research

The following overview compiles actual research areas of plant cell biology that have received substantial input by Ca²⁺- and H⁺-imaging experiments. After a short description of the state of the problem, actual concepts of cellular signalling are introduced that are influenced by imaging data.

Hormonal control of stomatal movements in guard cells

Stomatal movements represent controlled changes in guard cell turgor via mass fluxes of K⁺ and counteranions through ion channels of the plasma membrane and the tonoplast. These channels are targets of hormonetriggered signal chains (Blatt and Thiel 1993) that include shifts in cytoplasmic pH and Ca²⁺.

Abscisic acid triggers closing of stomata preceded by cytoplasmic alkalinization and an increase in cytoplasmic Ca²⁺ levels. These ionic transients were first detected by confocal imaging with BCECF or Fluo-3 of guard cells in epidermal strips of the orchid *Paphiopedilum tonsum* (Irving et al. 1992). Similar changes are known from ion maps obtained of maize coleoptiles and parsley hypocotyls and roots (Gehring et al. 1990b).

In contrast, auxin at low concentrations ($<100~\mu M$) causes stomatal opening which is preceded by cytosolic acidification, but likewise an increase in Ca_{cyt}^{2+} . This was imaged in the same experimental systems (Gehring et al. 1990b; Irving et al. 1992) and is in agreement with microelectrode measurements (Blatt and Armstrong 1993).

The signal character of pH shifts was seriously considered when their relationship to stomatal movements (acidification precedes opening and alkalinization precedes closing) was shown to reflect a pH-dependent control over K^+ channels of the plasma membrane.

Stomatal opening requires mass influx of K^+ via inwardly rectifying K^+ channels that are activated by increasing the cytosolic H^+ concentration (Blatt and Thiel 1994). In a combined assay of cytosolic pH (pH_{cyt}) via ratio photometry with BCECF and microelectrode measurements of K^+ current the protonation site of this channel could even be titrated in vivo with a pK_a near 6.3 (Grabov and Blatt 1997).

Conversely, stomatal closure involves K⁺ efflux via the outwardly rectifying K^+ channel, which is activated by decreasing cytosolic H^+ concentrations (Blatt and Armstrong 1993) with an apparent pKa of 7.4 (Grabov and Blatt 1997). Hence, the alkalinization caused by ABA can be expected to inhibit the K⁺-influx channels and activate the K⁺-efflux channel, thus promoting stomatal closure. The link between pH_{cvt} and K⁺-channel activity was further substantiated by combined pH mapping and voltage-clamp experiments with a synthetic peptide homolog of the C-terminus of the auxin-binding protein (ABP) from Zea mays (Thiel et al. 1993). This peptide mimicks the effect of high auxin concentrations (>100 μM), i.e. stomatal closing, reversible alkalinization in the cytoplasm (visualized by confocal pH mapping with BCECF) and a parallel, reversible inactivation of the inward rectifying K + channels. The latter inhibition was prevented by clamping pH_{cvt} to near 7.0 with butyric acid, irrespective of whether it was evoked by the above peptide (Thiel et al. 1993) or high auxin.

Mutations in the relevent gene (*abi-I*) provide ABA insensitivity to *Arabidopsis* guard cells by abolishing the response of K_{in} and K_{out} channels to ABA (Armstrong et al. 1995) and to experimental changes of pH_{cyt} (Blatt and Grabov 1997). These phosphatases are strongly activated by small pH increases like those evoked by ABA and require millimolar concentrations of Mg²⁺ for activity (Leube et al. 1998). They appear to be targets of the pH signal as well as of the Mg²⁺ status of the cytoplasm which they convert into K⁺ channel activity via a hitherto uncharacterized dephosphorylation step (Grill and Himmelbach 1998).

The K⁺-influx channels are also activated by extracellular (apoplastic) protons that are sensed by extracellular binding sites of the channel protein (Hoth et al. 1997). The well known H⁺ extrusion from auxin-treated cells might therefore be involved in the regulation of K⁺ influx. Imaging of the apoplastic pH with dextrancoupled pH probes (Taylor et al. 1996) offers a way to verify this hypothesis.

The signal character of Ca²⁺ in guard-cell movements has long remained obscure as the [Ca²⁺]_{cyt} is raised by different hormones irrespective of whether they cause stomatal opening (low IAA, kinetin, fusicoccin) or closing (ABA, high IAA, the C-terminal peptide of ABP). The inwardly transporting K⁺ channels of the plasma membrane, independent of their activation by cytosolic H⁺, are inactivated by cytosolic Ca²⁺ (ratio photometry with Fura-2 and BCECF together with microelectrode measurements, Grabov and Blatt 1997).

The outwardly transporting K^+ channel provides the major path for K^+ efflux during stomatal closure. This channel is known to be activated by decreasing $[H^+]_{cvt}$

(cf. above) but not directly influenced by [Ca²⁺]_{cyt} (Blatt and Armstrong 1993; Lemtiri-Chlieh and MacRobbie 1994; Grabov and Blatt 1997). It is, however, activated by depolarisation of the plasma membrane (Blatt and Armstrong 1993), an effect which indeed occurs during ABA treatment (Thiel et al. 1992).

Stimulation of K⁺ efflux via depolarization of the plasma membrane appears now to be a point of attack of several events that are mostly related to $[Ca^{2+}]_{cyt}$: first, anion efflux via Ca^{2+} -activated, slow-type anion channels leads to a sustained, long-term effect (e.g. Linder and Raschke 1992; Grabov et al. 1997); second, an initial, short-term depolarization caused by Ca² influx mainly through a voltage-gated, less-selective Ca²⁺ channel that is mediated by ABA (Schroeder and Hagiwara 1990). Actual imaging data indicate that oscillations of cellular Ca²⁺ provide the background for the tuning of ABA effects during stomatal closure. Combined ratio imaging with Fura-2 and voltage-clamp measurements in guard cells of Vicia (Grabov and Blatt 1998a) visualized a Ca²⁺ wave that could be triggered by experimental oscillations of membrane potential (negative of -120 mV) and moved from the periphery to the central part of the cytoplasmic/nuclear region. This wave most probably originated from an influx of Ca²⁺ as indicated by quenching of Fura-2 fluorescence after substituting external Mn²⁺ for Ca²⁺. Abscisic acid strongly shifted the voltage threshold for evoking the Ca²⁺ wave to less-negative values and increased both its amplitude and duration. While these data establish an important role for the membrane voltage in triggering and conditioning ABA-controlled oscillations of [Ca²⁺]_{cvt}, complementary experiments (whole-cell fluorescence ratioing of Fura-2) provide an idea of where such oscillations are positioned within the putative signal transduction chain(s) (Staxén et al. 1999). In guard cells of Commelina, ABA induced oscillations of [Ca²⁺]_{cyt} whose period (but not magnitude) depended on the hormone concentration and correlated with the resulting stomatal aperture. Both Ca²⁺ oscillations and stomatal closure were suppressed by a specific inhibitor of the phosphoinositide-converting phospholipase C. As Ca²⁺ oscillations that were triggered not by ABA but by raising the external Ca²⁺ (McAinsh et al. 1992, 1995) were not sensitive to the inhibitor, it is suggested that ABA-mediated imositol(1,4,5)triphosphate (IP₃) production and subsequent mobilization of endogenous Ca²⁺ are early steps of signalling that generate Ca²⁺ oscillations which in turn transduce the strength of the ABA signal into a steady state of stomatal aperture (Staxén et al. 1999).

The ABA-specific Ca²⁺ peaks or oscillations may originate from an influx of the external ion (Schroeder and Hagiwara 1990; Grabov and Blatt 1998a) but may also represent an efflux from vacuolar Ca²⁺ stores. These might be mobilized by interaction of cyclic ADP-ribose(CADPR) a central intermediate of ABA signalling (Wu et al. 1997) with ryanodine-sensitive Ca²⁺ channels of the tonoplast (Muir and Sanders 1996). Imositol(1,4,5)triphosphate is another Ca²⁺-mobilizing signal (cf. Staxén et al. 1999) in guard cells but it is not

clear whether it acts on vacuolar or other endogenous Ca²⁺ stores. The mobilization of intracellular Ca²⁺ stores is likely to be a point of interaction of Ca²⁺ and H⁺-mediated signalling: an experimental decrease in pH_{cvt} below 7.0 led in guard cells to an elevation of Ca²⁺ (Grabov and Blatt 1997), most probably via the H⁺-dependent gating of vacuolar ion channels (Schulz-Lessdorf and Hedrich 1995).

Summarizing, ABA signalling in guard cells appears to follow a bifurcated signal path that contains both a Ca²⁺-dependent and a Ca²⁺-independent, pH-controlled branch (Grabov and Blatt 1997, 1998a,b; Grill and Himmelbach 1998). Both branches might interact at later stages of signalling, thereby generating the complex shifts of Ca²⁺ concentration termed the ABA-specific Ca²⁺-signature (cf. below).

Signalling by gibberellic and abscisic acid in aleurone cells

Cereal aleurone cells respond to gibberellins (GA₃) with the production and secretion of several hydrolases (mainly α-amylases) and vacuolation. The earliest events measured after hormone contact are an increase in cytoplasmic Ca²⁺ and H⁺ as well as calmodulin (for a recent review cf. Bethke et al. 1997). The Ca²⁺ shift has been best characterized in barley aleurone protoplasts using ratiometric Ca²⁺ imaging with the probes Fluo-3, Indo-1 (loaded at low external pH), or Indo-1 dextran (loaded by microinjection, Gilroy and Jones 1992; Bush 1996; Gilroy 1996). These maps reveal that GA₃ evokes a sustained increase in Ca²⁺ mainly in the peripheral cytoplasm which is consistent with the earlier idea of an Ca²⁺ influx via plasma-membrane channels (Schroeder and Hagiwara 1990).

The effect of GA₃ on Ca²⁺ levels could be antagonized by subsequent addition of ABA, which reflects the mutual antagonism of the two hormones with respect to the secretory response (Gilroy 1996). Cytoplasmic Ca²⁺ was experimentally increased by microinjection of either CaCl₂ or caged Ca²⁺, from which sequential Ca²⁻ peaks were liberated by UV pulses (Gilroy 1996). These Ca²⁺ shifts alone, as well as microinjection of barley calmodulin proved insufficient to mimick the action of GA₃. On the contrary, injection of Ca²⁺-binding buffers blocked the GA₃-induced secretion of α-amylases but not the induction of the α -amylase gene. It was therefore concluded that increased [Ca²⁺]_{cyt} is required for the functioning of the secretory mechanism, but is not a direct intermediate of GA₃-triggered gene expression (Gilroy 1996; Bethke et al. 1997). A pH response to GA₃ of aleurone cells has so far been demonstrated only by a null-point method that measures pH changes of weakly buffered external media caused by digitonin permeabilization of the plasma membrane (Heimovaara-Dijkstra et al. 1994). pH mapping in these cells, i.e. visualization of the spatial dimension of the expected pH decrease by a less-invasive method remains to be done.

The cytoplasmic acidification caused by GA₃ has been imaged in maize coleoptile cells by a careful

confocal study with the probes BCECF and cSNARF-1, and proved to be similar to the effects of auxin (Gehring et al. 1994). Furthermore, GA_3 triggers vacuolar acidification in aleurone cells (a prerequisite for the activation of vacuolar proteases that mobilize storage proteins) by influencing the activity but not the numbers of tonoplast H^+ pumps (measured with BCECF, Swanson and Jones 1996).

Targets of the pH shift in the course of GA_3 signalling have not yet been identified. An influence of artificial shifts in pH_{cyt} on the induction of the intact α -amylase promoter could not be established (Heimovaara-Dijkstra et al. 1995). Interestingly, a chimeric α -amylase promoter construct containing several GA_3 -responsive elements was induced by lowering pH_{cyt} . On the other hand, induction of a promoter of the Rab gene family in the presence of ABA was enhanced by a pH increase of magnitude similar to that caused by ABA (Heimovaara-Dijkstra et al. 1995). It seems, therefore, that pH_{cyt} is not a sufficient signal but a factor influencing the efficiency of ABA-controlled gene expression in aleurone cells.

Elicitation of antimicrobial defenses

Contact with elicitor molecules (distinct glycoproteins, oligosaccharides or proteins of pathogenic microorganisms) evokes a complex variety of defense responses in plant cells. The earliest reactions are perturbations of the cellular ionic balance, i.e. efflux of K⁺ and Cl⁻, influx of Ca²⁺, external alkalinization and cellular acidifcation (e.g. Mathieu et al. 1991) and an oxidative burst, i.e. the extracellular generation of reactive oxygen species by a plasma-membrane NADPH-oxidase (cf. Lamb and Dixon 1997 for a recent review). They may be followed by oxidative cross-linking of cell-wall constituents, overproduction of plant phenolics, hypersensitive cell death and induction of several genes. Integrative signal systems obviously coordinate such responses at the cellular and the systemic level (Levine et al. 1994; Kombrink and Somssich 1995; Jabs et al. 1997; Ebel and Mithöfer 1998) but allow autonomous expression of distinct branches of signal chains including the species-specific formation of phytoalexins. Shifts in Ca2+1 and of H+ concentrations appear to act as early signal intermediates, though at different levels of complexity.

A pulse of cytoplasmic Ca²⁺ following elicitor contact was first shown by the aequorin method (Knight et al. 1991) and is most probably due to activation of plasma-membrane Ca²⁺ channels (Zimmermann et al. 1997). It seems to transduce the elicitor signal towards the NADPH-oxidase as judged from appropriate effects on this enzyme activity of Ca²⁺ buffers and injection of external Ca²⁺ (Chandra and Low 1997). In addition, Ca²⁺ might have a signal function downstream of the oxidative burst in connecting it to the cell death program (Levine et al. 1996; Lamb and Dixon 1997).

Cytoplasmic acidification was frequently observed in elicitor treated plant cells (Mathieu et al. 1991, 1996a;

Roos 1992; Kuchitsu et al. 1997; Roos et al. 1998) and appears to be involved in different signal chains and to have different origins. Under conditions that allow the hypersensitive reaction, cytoplasmic acidification is tightly coupled to an alkalinization of the outer medium, indicating an influx of external protons (Mathieu et al. 1991, Kuchitsu et al. 1997). Such a process has been detailed by monitoring the distribution of [14C] benzoic acid in tobacco cells that responded to oligogalacturonide elicitors (Mathieu et al. 1996a). Inhibitor experiments point to a phosphorylation-dependent control of this proton influx (Mathieu et al. 1996b).

In contrast, the selective elicitation of benzophenanthridine alkaloids, phytoalexins of Eschscholzia californica, neither required an alkalinization of the outer medium nor was it linked to an oxidative burst. Cultured cells reacted to low concentrations of a yeast glycoprotein elicitor with a rapid, transient acidification of the cytoplasm and a concomitant increase in the vacuolar pH, as shown by confocal pH mapping with cSNARF-1 (Roos et al. 1998; Fig. 3). Quantitation of the pH maps revealed a nearly constant proportion between the concentration of protons disappearing from the vacuole and those arriving in the cytoplasm, suggesting an efflux of H⁺ from the vacuole and a constant buffering capacity of the cytoplasm. pH mapping also allowed controlled gain- and loss-of-function experiments that corroborated the signal character of cytoplasmic pH shifts: artificial acidification with butyric acid triggered alkaloid biosynthesis, whereas treatment with strong buffers or methylamine at $pH_{ext} = 7.4$ led to the reversible deprivation of vacuolar acidity and prevented the effects of elicitors on alkaloid biosynthesis. It appears, therefore, that a transient cytoplasmic acidification provided by vacuolar protons is a necessary step of the signal path towards phytoalexin formation (Roos et al. 1998). A vacuolar origin of cytoplasmic pH shifts has also been suggested in guard-cell protoplasts where the auxin-triggered acidification of the cytoplasm was absent after evacuolation, though the characteristic stimulation of H⁺ secretion was retained (Frohnmeyer et al. 1998).

Calcium as a universal signal molecule in plant cells

During the last decade, shifts in the cellular distribution of ${\rm Ca}^{2^+}$ have been identified as an intermediate step in a wide variety of plant signalling pathways and have thus turned out to act as intermediates of environmental responses as well as of developmental programs (cf. Trewavas and Malhó 1998 for a recent review). The following examples demonstrate the enormous heterogeneity of ${\rm Ca}^{2^+}$ transients in plant cells.

(i) Apical growth and cell polarity. Calcium plays a fundamental role in the control of polarized growth in apically growing cells. A tip-focused, steep gradient of cytoplasmic Ca²⁺ is a common feature of such cells and has been imaged in pollen tubes (Fura-2-dextran, Pierson et al. 1996), root hairs (confocal imaging with Indo-1, Wymer et al. 1997), and *Fucus* rhizoid cells

(confocal imaging with Calcium Green-dextran, Berger and Brownlee 1993). It derives from Ca²⁺ entry via clustered Ca²⁺ channels in the apical region of the plasma membrane (Pierson et al. 1996; Taylor et al. 1997; Wymer et al. 1997) that acts in concert with unknown, endogenous polarity-determining factors (Bibikova et al. 1997). The apical Ca²⁺ gradient, which is a prerequisite of directed growth (Malho et al. 1995; Malho and Trewavas 1996; Trewavas and Malho 1997), shows characteristic oscillations that have been imaged with Fura-2 dextran (Franklin-Tong et al. 1997). Changes in this gradient are obviously involved in a number of responses to extracellular signals.

- (ii) Self-incompatibility response. In pollen tubes of *Papaver rhoeas*, Ca²⁺ waves take part in the prevention of self-fertilization which is achieved by the interaction of S-proteins specific to the pollen grain with those specific to the pistil. Whereas compatible S-proteins cause no changes in pollen-tube Ca²⁺, incompatible S-proteins trigger a gradual disappearance of the Ca²⁺ gradient at the tip and a fast increase in the sub-apical region followed by the inhibition of pollen tube growth (Franklin-Tong et al. 1997).
- (iii) Fertilization. The contact of distinct pollen types with the papillae of *Brassica napus* results in small peaks of papillar [Ca²⁺]_{cyt} as imaged with Calcium Greendextran. This response precedes the hydration of the applied pollen grains and is therefore considered to be a prerequisite of successful pollination (Dearnaley et al. 1997).
- (iv) Rhizobium nodulation signals. In alfalfa root hairs the contact with specific Nod factors (lipochitooligosaccharides) of the symbiont *Rhizobium meliloti* initiates oscillations of [Ca²⁺] (visualized with Calcium Green-dextran) with a main period of 60 s. Ratio imaging with Fura-2-dextran revealed that the Ca²⁺ spikes originated near the nucleus and migrated centrifugally (Ehrhardt et al. 1996). The signal character of these oscillations with respect to the following nodule development is supported by their absence in a non-nodulating mutant and by identical structural requirements of both the nodulation- and the Ca²⁺-response for active Nod signal molecules.
- (v) Osmotic control of cell volume. Hypoosmotic shock triggers in *Fucus* rhizoid cells a rapid, transient increase in $[Ca^{2+}]_{cyt}$ propagating from the apex to subapical regions. In the absence of this transient, i.e. during a refractory period between successive hypoosmotic shocks or after microinjection of Ca^{2+} buffers, the cells are unable to osmoregulate and undergo osmotic burst. Complementing data from Ca^{2+} -ratio imaging with Fura-2 and patch-clamp experiments at localized areas of the plasma membrane suggest that at least some of the Ca^{2+} channels of the apex region are stretch-activated and involved in the measured Ca^{2+} peak (Taylor et al. 1996).

In contrast, hydration of the cytoplasm of *Nitella flexilis* via perfusion of the vacuole with hypotonic media triggers a release of cytolasmic Ca²⁺ from internal stores as detected in aequorin-loaded cells (Tazawa et al. 1995).

- (vi) Phototropic and gravitropic responses. In maize coleoptiles loaded with Fluo-3 AM, light and gravity induced an asymmetric distribution of Ca²⁺ with higher concentrations at the shaded side or the lower side of horizontally placed cotyledons, respectively. It is suggested that these shifts are instrumental to later changes in the distribution of auxin-regulated mRNAs (Gehring et al. 1990a). In gravistimulated roots, however, no Ca²⁺ shifts have been detected as yet (Legué et al. 1997).
- (vii) Carbon dioxide. In stomatal guard cells of epidermal strips of *Commelina communis*, elevated CO₂ concentrations triggered a reversible increase in Ca²⁺ as measured by ratio photometry of Fura-2 fluorescence. This response showed characteristics similar to the reaction to ABA and required the presence of extracellular Ca²⁺ (Webb et al. 1996).

(viii) Touch. In roots of *Arabidopsis* Ca²⁺-imaging with Indo-1 revealed touch-elicited transients of [Ca²⁺]_{cyt} that were most pronounced in the cap cells. The inhibitory effect of ruthenium red, an inhibitor of mitochondrial Ca²⁺ channels argued for the involvement of intracellular sites of Ca²⁺ release (Legué et al. 1997). Touch-induced spikes of cytosolic Ca²⁺ are also known from tobacco seedlings expressing aequorin (Knight et al. 1991).

The following examples indicate how the use of transgenic aequorin has promoted the detection of calcium peaks in whole plants and seedlings under a variety of stimuli.

- (i) Oxidants. Hydrogen peroxide causes a transient increase in [Ca²⁺]_{cyt} in *Nicotiana* seedlings followed by a refractory period of several hours (Price et al. 1994).
- (ii) Anoxia. Withdrawal of oxygen causes a biphasic response of $[Ca^{2+}]_{cyt}$ in cotyledons and leaves of *Arabidopsis* seedlings. Calcium-channel blockers such as Gd^{3+} , La^{3+} , and ruthenium red inhibit the first luminescence peak, which arises within a few minutes, but promote the second peak that appears after 1.5–4 h, thus suggesting the involvement of different cellular Ca^{2+} sources (Sedbrook et al. 1996).
- (iii) Cold shock. Addition of ice-cold water to individual seedlings evokes a sudden rise in $[Ca^{2+}]_{cyt}$ that requires both Ca^{2+} influx through the plasma membrane and efflux from vacuolar Ca^{2+} stores (Knight et al. 1996). In these studies, aequorin was expressed either in the cytosol (*Arabidopsis* and *Nicotiana*) or at the cytoplasmic surface of the vacuolar membrane (fusion protein with the vacuolar pyrophosphatase of *Arabidopsis*).

The above examples demonstrate the involvement of Ca²⁺-shifts in a multitude of signal pathways that lead to very different or even opposing responses. Thus, the messages carried by the cellular Ca²⁺ signal are encoded not only by the change in concentration but include a great variety of time- and space-dependent elements. First of all, Ca²⁺ shifts occur at different levels of magnitudes: guard cells responded to the auxin 2,4,-dichlorophenoxy acetic acid (2,4-D) by increasing [Ca²⁺]_{cyt} from 280 nM to 380 nM (Gehring et al. 1990a) and to ABA by variable increments ranging from 100 to 750 nM (McAinsh et al. 1992), whereas tips

of growing pollen tubes showed oscillations of [Ca²⁺]_{cvt} between 700 nM and 10 µM (Trewavas and Malho 1998) and reacted, for example, to incompatible S proteins by raising [Ca²⁺] in some regions from 210 nM to $> 1.5 \mu M$ (Franklin-Tong et al. 1997). Variations of Ca²⁺ in time include sustained plateaus, single transients of different shape, oscillations and waves (Lipp and Bootman 1999). Frequencies and/or amplitudes of Ca²⁺ messages can indeed be sensed and discriminated by cellular targets. This has been shown for animal cells, e.g. for IP₃-triggered Ca²⁺ oscillations that activate mitochondrial metabolism (Hajnocky et al. 1995; Hajnocky and Thomas 1997) and for the different modes of Ca²⁺-activation of the transcription factors $NF\kappa B$, NFAT and JNK (Dolmetsch et al. 1997). Frequency-encoded Ca²⁺ signals have recently been observed in ABA-treated guard cells (Staxén et al. 1999). Potential generators of Ca²⁺ fluctuations in the plant cell are Ca²⁺ channels that allow various modes of release from and uptake into intracellular stores as well as influx of external calcium. Calcium fluxes across the plasma membrane can be triggered by membrane hyperpolarization as shown not only in guard cells (e.g. Grabov and Blatt 1998a) but also by depolarization, as in the carrot cell plasma membrane (Thuleau et al. 1994), or mechanical stress (Taylor et al. 1996). Intracellular Ca²⁺ fluxes which can originate from the vacuole and/or other, hitherto ill-defined, intracellular stores are controlled by IP₃ (Knight et al. 1997; Staxén et al. 1999), cADPR (Muir and Sanders 1996) or by the cytoplasmic Ca²⁺ concentration that acts on slow vacuolar channels leading to Ca²⁺ efflux (Ward et al. 1995; Allen and Sanders 1996). The latter case might give rise to a Ca²⁺-induced Ca²⁺ release (CICR) which is likely to play a role in the formation of Ca²⁺ spikes that direct the growth of pollen tubes (Malho et al. 1995; Trewavas and Malho 1997).

The involvement of different intracellular stores appears a major element in the spatial variation of Ca²⁺ transients. For instance, cold shock, touching or oxidant contact seem to mobilize different pools of calcium (Price et al. 1994). The extent of Ca²⁺ shifts in the cytosol may be further controlled by the cytoskeleton, as judged from increased calcium responses to cold shock after treatment with drugs impairing microtubules or microfilaments (Mazars et al. 1997). Such data further argue for an influence of cytoskeletal structures on the spatial patterns of cytosolic Ca²⁺ transients. Summarizing, Ca²⁺ signalling in plant cells both obeys and changes a cell- and stage-specific distribution of this ion, i.e. a Ca²⁺ landscape with a dynamic topology. Each external signal introduces unique changes into this landscape that have been termed the calcium signature (Knight et al. 1996; McAinsh et al. 1997; Trewavas and Malhó 1998). Such signatures allow much more information to be transmitted than a simple transient alone and might also allow memory effects: pretreatment of seedlings with cold or hydrogen peroxide (acclimation) resulted in a modified Ca²⁺ signature to subsequent cold shock (Knight et al. 1996).

Cytosolic pH and cellular development

A gradient of cytosolic pH has been implicated in the regulation of polarized growth in plant and fungal cells. However, evidence of such a gradient in tip-growing cells remains contradictory if recent confocal imaging data are compared. Gibbon and Kropf (1994) have seen a longitudinal pH gradient in rhizoid cells of Pelvetia embryos (0.3–0.5 pH units, with the apical cytosol more acidic) by imaging with dextran-conjugated cSNARF-1 and confirmed it by microelectrode measurements. The magnitude of this gradient correlated well with the rate of elongation growth and both parameters were strongly reduced by treatment with membrane-permeant acids (Kropf et al. 1995). In contrast, Bachewich and Heath (1997) did not find a cytoplasmic pH gradient by imaging hyphal cells of the oomycete fungus Saprolegnia ferax with acid-loaded cSNARF-1. Nevertheless, experimental acidification of pH_{cvt} to 6.8 by permeant acids caused reversible inhibition of tip growth together with alterations in the cytoskeletondependent organization of tip morphology (including relocation of mitochondria and condensation of chromatin), thus implying a role for H⁺ in regulating growth-correlated activities.

Parton et al. (1997), in an extended imaging study with AM-ester and dextran-conjugated cSNARF-1, did not see cytoplasmic pH gradients > 0.1 units in tip-growing cells of Neurospora, pollen tubes of Agapanthus umbellatus and rhizoids of Dryopteris affinis gameto-phytes. Again, artificial acidification of the cytoplasm to a pH near 7 reduced (Neurospora) or completely inhibited (Agapanthus and Dryopteris) apical growth. Pollen tubes of Lilium longiflorum did not display a consistent pH gradient in the growth zone (ratio imaging with BCECF). Growth stopped upon increasing pH_{cyt} by either external alkalinization or inhibition of the plasma-membrane H⁺-ATPase by vanadate, and also by adding Ca²⁺ or La³⁺ (Fricker et al. 1997).

The above data exemplify the intriguing problem around the signal character of ΔpH in growth and developmental regulation: though indications of pHsensitive steps exist – usually deduced from the effects of artificial pH shifts - proton transients that appear sufficient for such purposes are not always detectable in vivo. Seen apart from methodical problems (e.g. dye exclusion from vesicles stacking at apical regions or poor resolution of such microcompartments), some pecularities of cellular H⁺ management must be taken into account that might obscure the detection of proton gradients: (i) the magnitude of pH shifts of regulatory significance might be close to or below the detection limit of the used mapping procedure; (ii) they might be highly localized, i.e. associated with the plasma membrane or other organelles; and (iii) they might display non-synchronous oscillations and other time-dependent

The reported H⁺ gradients are generally smaller than those frequently found in Ca²⁺ signalling. If one realizes the 10-fold higher diffusion coefficient of H₃O⁺ com-

pared to Ca²⁺ and the high efficiency of cytoplasmic pH homeostasis, it appears very likely that H⁺ gradients last relatively briefly and are often visible only in close proximity to the sites of proton generation or loss. Such local domains of different pH are likely to be established by oscillations of proton pumping, passive H⁺-transports and the biochemical pH-stat which show different frequencies (Shabala et al. 1997), and by the inhomogeneous distribution of H⁺-buffering capacities, including those that are connected to the cytoskeleton. Examples are the acidic regions of the cytoplasm close to the plasma membrane as they have been imaged in cultured plant cells and fungal protoplasts (Roos 1992). Electron transfer across the plasma membrane is another potential source of local cytoplasmic acidification (Pönitz and Roos 1994). The large proton pool of the plant vacuole very effectively contributes to the pHhomeostasis of the cytoplasm: pH changes connected with the uptake of NH₃ are almost fully compensated by vacuolar accumulation with fewer effects on pH_{cvt} (Brauer et al. 1997; Roos et al. 1998); acid loads imposed by permeant acids have much lower impact on pH_{cvt} if the vacuolar pumps are active (Frohnmeyer et al. 1998; Roos et al. 1998). Thus, while cytoplasmic pH transients are minimized by various buffers the loss of vacuolar protons at the same time can be taken as another indication of proton fluxes into the cytoplasm (Roos et al. 1998).

Changes in cytoplasmic pH (both natural and artificial) can mobilize Ca²⁺ from intracellular (e.g. vacuolar) stores and thus create points of interaction between H⁺ and Ca²⁺ signalling (Felle 1988; Guern et al. 1992; Grabov and Blatt 1997, 1998b). The Ca²⁺ reservoir of the cell wall may also be mobilized by H⁺ extrusion as suggested from strongly synchronized oscillations between H⁺ and Ca²⁺ fluxes that occur around the elongation region of maize roots (Shabala et al. 1997). Hence, when putative regulatory functions of identified pH gradients are considered, the possibility of interacting with Ca²⁺ gradients should be investigated, for instance by parallel imaging of Ca²⁺ and H⁺.

Summarizing, in the near future proton signalling could prove as subtle as the Ca²⁺ information but with differing characteristics. It seems realistic to expect cellular H⁺ signatures that provide and connect fast signalling events at distinct microenvironments and thereby complement the longer-lasting Ca²⁺ signature.

Outlook: future tasks and challenges of ion imaging

Despite their actual limitations, ion-imaging procedures have demonstrated the potential to visualize space- and time-coded patterns of Ca²⁺ and H⁺ distribution in a large variety of plant cells. There is growing evidence that the final intracellular message initiated by a distinct environmental or developmental stimulus is not a one-way sequence but rather a specific combination of activated ion channels, protein kinases, protein phosphatases, phospholipases or other stimulus-response couplers. Such a signalling network is very

likely to include the distinct signatures of Ca²⁺, H⁺ and membrane potential, and may include other ions like Na⁺ and Mg²⁺. Unraveling the topography, generators and addresses of peaks, oscillations, waves and other patterns of ion distribution therefore becomes a central task in signal transduction research. This creates the necessity to obtain more quantitative, statistically sound data rather than qualitative or semi-quantitative measurements that actually dominate imaging experiments with plant cells. Furthermore, it becomes clear that concerted approaches that monitor more than one signal parameter (e.g. ion imaging combined with electrophysiological measurements in whole cells, Grabov and Blatt 1997, 1998a; simultaneous imaging of Ca²⁺ and H⁺, see below) have the best chances of finding causal relationships and signal sequences within these complexities.

With regard to methodical constraints, the following, hitherto unresolved problems are among the targets, expectations and challenges of the near future.

Ion contents of small organelles. New developments in confocal, lifetime and two-photon imaging can be expected to improve the resolution and alignment of imaging information with subcellular structures such as the vesicular and reticular organelles of the plant cell including mitochondria that are often stacked at high densities. Fluorescence or luminescence signals of defined organellar origin are the goal of designing organelle-specific fluorescent probes whether it be by liposome-based targeting or by the site-directed expression of aequorins and pH-sensitive GFPs. Advances in the molecular design of expression vectors with varying targeting sequences and improved transgenic technologies will allow new experimental approaches for the simultaneous visualization/quantification of ion concentrations in different organelles.

Simultaneous imaging of different probes - crosstalk of H^+ - and Ca^{2+} -signalling. Simultaneous imaging of Ca2+ and H+ has mainly been exercised with animal cells. As an example, in cultured renal epithelial cells loaded with Indo-1 plus cSNARF-1, ratio imaging revealed that arginine vasopressin caused not only changes in pH_{cyt} that are modified by Ca^{2+} but also changes in Ca^{2+} that are not modified by ΔpH (Vamos et al. 1997). In plant cells this technique is not yet in routine use due to the difficulty of separating the emission signals of different probes and adjusting as well as calibrating them to the dynamic range of the optical system. Modern confocal microscopes will facilitate these tasks as they allow the generation of fluorescence spectra of distinct cellular areas. Simultaneous imaging can help to establish the long-assumed interactions of H⁺ and Ca²⁺ transients (cf. above) and to prove a putative crosstalk between the two signal paths at different cellular locations, including the cell wall.

Complementing microscopic techniques. In recent years, several fluorescence and electron-microscopic techniques

have been put forward that can effectively complement ion imaging in the investigation of complex signal transfer processes at the single-cell level. For instance, imaging of free and bound calmodulin – an important extension of Ca²⁺ imaging – can be achieved via fluorescence resonance energy transfer (FRET). The interaction of the eukaryotic elongation factor 1-α (EF1-α), calmodulin, and cytoskeletal elements has already been demonstrated by this technique (e.g. Durso and Cyr 1994), which can also be adapted to image cAMP (Adams et al. 1991) and various enzyme activities. Monitoring of FRET can be substantially improved by fluorescence lifetime imaging as this makes it independent of the concentration and intensity of the donor compound (Gadella 1999).

Fluorescence polarisation anisotropy likewise appears a good candidate for imaging small, non-ionic signal molecules interacting with cellular structures. Last but not least, electron microscopy is now able to image very small amounts of metals and other elements in biological specimens, e.g. by electron spectroscopic imaging (ESI) and contrast analysis (Kortje 1996).

References

Adams SR, Harootunian AT, Buechler YJ, Taylor SS, Tsien RY (1991) Fluorescence ratio imaging of cyclic AMP in single cells. Nature 349: 694–697

Agard DA, Hiraoka Y, Shaw P, Sedat JW (1989) Fluorescence microscopy in three dimensions. Methods Cell Biol 30: 353–377

Allen GJ, Sanders D (1996) Control of ionic currents in guard cell vacuoles by cytosolic and luminal calcium. Plant J 10: 1055–1069

Armstrong F, Leung J, Grabov A, Brearley J, Giraudat J, Blatt MR (1995) Sensitivity to abscisic acid of guard-cell K⁺ channels is suppressed by *abi1-1*, a mutant *Arabidopsis* gene encoding a putative protein phosphatase. Proc Natl Acad Sci USA 92: 9520–9524

Ashley RH (1986) Buffer capacity of intracellular calcium indicators. Biochem J 240: 310–311

Bachewich CL, Heath IB (1997) The cytoplasmic pH influences hyphal tip growth and cytoskeleton related organization. Fungal Genet Biol 21: 76–91

Berger F, Brownlee C (1993) Ratio confocal imaging of free cytoplasmic calcium gradients in polarizing and polarized *Fucus* zygotes. Zygote 1: 9–15

Bethke PC, Schuurink RC, Jones RL (1997) Hormonal signalling in cereal aleurone. J Exp Bot 48: 1337–1356

Bibikova TN, Zhigilei A, Gilroy S (1997) Root hair growth in *Arabidopsis thaliana* is directed by calcium and endogenous polarity. Planta 203: 495–505

Blatt MR, Armstrong F (1993) K⁺ channels of stomatal guard cells: abscisic acid-evoked control of the outward rectifier mediated by cytoplasmic pH. Planta 191: 330–341

Blatt MR, Grabov A (1997) Signalling gates in abscisic acidmediated control of guard cell ion channels. Physiol Plant 100: 481–490

Blatt M, Thiel G (1993) Hormonal control of ion channel gating. Annu Rev Plant Physiol Plant Mol Biol 44: 543–567

Blatt MR, Thiel G (1994) K⁺ channels of stomatal guard cells: bimodal control of the K⁺ inward-rectifier evoked by auxin. Plant J 5: 55–68

Boyarsky G, Hanssen C, Clyne LA (1996a) Inadequacy of high K ⁺ nigericin for calibrating BCECF. I. Estimating steady-state intracellular pH. Am J Physiol 271: C1131–C1145

- Boyarsky G, Hanssen C, Clyne LA (1996b) Superiority of in vitro over in vivo calibrations of BCECF in vascular smooth muscle cells. FASEB J 10: 1205–1212
- Brauer D, Otto J, Tu S-I (1995) Selective accumulation of the fluorescent pH indicator, BCECF, in vacuoles of maize roothair cells. J Plant Physiol 145: 57–61
- Brauer D, Uknalis J, Triana R, Tu S-I (1996) Subcellular compartmentation of different lipophilic fluorescein derivatives in maize root epidermal cells. Protoplasma 192: 70–79
- Brauer D, Uknalis J, Triana R, Tu S-I (1997) Effects of external pH and ammonium on vacuolar pH in maize root hair cells. Plant Physiol Biochem 35: 31–39
- Brezden CB, Hedley DW, Rauth AM (1994) Constitutive expression of P-glycoprotein as a determinant of loading with fluorescent calcium probes. Cytometry 17: 343–348
- Brini M, Marsault R, Bastianutto C, Pozzan T, Rizzuto R (1994) Nuclear targeting of aequorin – a new approach for measuring nuclear Ca²⁺ concentrations in intact cells. Cell Calcium 16: 259–268
- Bush DS (1996) Effects of gibberellic acid and environmental factors on cytosolic calcium in wheat aleurone cells. Planta 199: 80–90
- Carrington WA, Lynch RM, Moore EDW, Isenberg G, Fogarthy KE, Fay SF (1995) Superresolution three-dimensional images of fluorescence in cells with minimal light exposure. Science 268: 1483–1487
- Chae Q, Park HJ, Hong SD (1990) Loading of quin2 into the oat protoplast and measurement of cytosolic calcium ion concentration changes by phytochrome action. Biochim Biophys Acta 1051: 115–122
- Chandra S, Low PS (1997) Measurement of Ca²⁺ fluxes during elicitation of the oxidative burst in aequorin-transformed tobacco cells. J Biol Chem 272: 28274–28280
- Cody SH, Dubbin PN, Beischer AD, Duncan ND, Hill JS, Kaye AH, Williams DA (1993) Intracellular pH mapping with SNARF-1 and confocal microscopy: I. A quantitative technique for living tissues and isolated cells. Micron 24: 573–580
- Coleman JOD, Randall R, Blakekalff MMA (1997) Detoxification of xenobiotics in plant cells by glutathione conjugation and vacuolar compartmentalization: a fluorescent assay using monochlorobimane. Plant Cell Environ 20: 449–460
- Cork RJ (1986) Problems with the application of quin-2-AM to measuring cytoplasmic free calcium in plant cells. Plant Cell Environ 9: 157–161
- Crawford LA, Bown AW, Breitkreuz KE, Guinel FC (1994)
 The synthesis of gamma-aminobutyric acid in response to
 treatments reducing cytosolic pH. Plant Physiol 104: 865–
 871
- Dearnaley JDW, Levina NN, Lew RR, Heath IB, Goring DR (1997) Interrelationships between cytoplasmic Ca²⁺ peaks, pollen hydration and plasma membrane conductances during compatible and incompatible pollinations of *Brassica napus* papillae. Plant Cell Physiol 38: 985–999
- Dolmetsch RE, Lewis RS, Goodnow CC, Healy JI (1997) Differential activation of transcription factors induced by Ca²⁺ response amplitude and duration. Nature 386: 855–858
- Dudler R, Hertig C (1992) Structure of an *mdr*-like gene from *Arabidopsis thaliana*: evolutionary implications. J Biol Chem 267: 5882–5888
- Durso NA, Cyr RJ (1994) A calmodulin-sensitive interaction between microtubules and a higher plant homolog of elongation factor-1 alpha. Plant Cell 6: 893–905
- Ebel J, Mithöfer A (1998) Early events in the elicitation of plant defense. Planta 206: 335–348
- Ehrhardt DW, Wais R, Long SR, Hughes H (1996) Calcium spiking in plant root hairs responding to *Rhizobium* nodulation signals. Cell 85: 673–681
- Felle H (1987) Proton transport and pH control in *Sinapis alba* root hairs: a study carried out with double-barrelled pH microelectrodes. J Exp Bot 38: 340–354

- Felle H (1988) Cytoplasmic free calcium in *Riccia fluitans* L. and *Zea mays* L.: Interaction of Ca²⁺ and pH? Planta 176: 248–255
- Floto RA, Mahaut-Smith MP, Somasundaram B, Allen JM (1995) UgG-induced Ca²⁺ oscillations in differentiated U937 cells; a study using laser scanning confocal mycroscopy and co-loaded Fluo-3 and Fura-Red fluorescent probes. Cell Calcium 18: 377– 389
- Franklin-Tong VE, Hackett G, Hepler PK (1997) Ratio-imaging of Ca_i²⁺ in the self-incompatibility response in pollen tubes of *Papaver rhoeas*. Plant J 12: 1375–1386
- Fricker MD, Tester M, Gilroy S (1993) Fluorescence and luminescence techniques to probe ion activities in living plant cells. In: Mason WT (ed) Fluorescent and luminescent probes for bilogical activity. Academic Press, London, pp 360–377
- Fricker MD, White NS, Thiel G, Millner P, Blatt MR (1994a)
 Peptides derived from the auxin-binding protein elevate Ca²⁺
 and pH in stomatal guard cells of *Vicia faba*: a confocal
 fluorescence ratio imaging study. In: Blatt MR, Leigh RA,
 Sanders D (eds) Membrane transport in plants and fungi:
 molecular mechanisms and control. SEB Symposium Series 48,
 Company of Biologists, Cambridge, pp 215–228
- Fricker MD, Tlalka M, Ermantraut J, Obermeyer G, Dewey M, Gurr S, Patrick J, White NS (1994b) Confocal fluorescence ratio imaging of ion activities in plant cells. Scanning Microsc 8: 391–405
- Fricker MD, White NS, Obermeyer G (1997) pH gradients are not associated with tip growth in pollen tubes of *Lilium longiflorum*. J Cell Sci 15: 1729–1740
- Fricker MD, Plieth C, Knight H, Blancaflor E, Knight MR, White NS, Gilroy S (1999) Fluorescence and luminescence techniques to probe ion activities in living plant cells. In: Mason WT (ed) Fluorescent and luminescent probes for bilogical activity, 2nd edn. Academic Press, San Diego, pp 570–596
- Frohnmeyer H, Grabov A, Blatt MR (1998) A role for the vacuole in auxin-mediated control of cytosolic pH by *Vicia* mesophyll and guard cells. Plant J 13: 109–116
- Gadella TWJ (1999) Fluorescence lifetime imaging microscopy (FLIM): Instrumentation and applications. In: Mason WT (ed) Fluorescent and luminescent probes for biological activity, 2nd edn. Academic Press, San Diego, pp 570–596
- Gehring CA, Williams DA, Cody SH, Parish RW (1990a) Phototropism and geotropism in maize coleoptiles are spatially correlated with increases in cytosolic free calcium. Nature 345: 528–530
- Gehring CA, Irving HR, Parish RW (1990b) Effects of auxin and abscisic acid on cytosolic calcium and pH in plant cells. Proc Natl Acad Sci USA 87: 9645–9649
- Gehring CA, Irving HR, Parish RW (1994) Gibberellic acid induces cytoplasmic acidification in maize coleoptiles. Planta 194: 532–540
- Gerritsen HC, Sanders R, Draaijer A (1994) Confocal fluorescence lifetime imaging of ion concentrations. Proc SPIE-Int Soc Opt Eng 2329: 260–267
- Gibbon BC, Kropf DL (1994) Cytosolic pH gradients associated with tip growth. Science 263: 1419–1421
- Giglioli-Guivarc'h N, Pierre JN, Vidal J, Brown S (1996) Flow cytometric analysis of cytosolic pH of mesophyll cell protoplasts from the crabgrass *Digitaria sanguinalis*. Cytometry 23: 241–249
- Gillot I, Whitaker M (1993) Imaging calcium waves in eggs and embryos. J Exp Biol 184: 213–219
- Gilroy SG (1996) Signal transduction in barley aleurone protoplasts is calcium dependent and independent. Plant Cell 8: 2193–2209
- Gilroy SG, Jones RL (1992) Gibberellic acid and abscisic acid coordinately regulate cytoplasmic calcium and secretory activity in barley aleurone protoplasts. Plant Biol 89: 3591–3595
- Gilroy SG, Hughes WA, Trewavas AJ (1989) A comparison between Quin-2 and aequorin as indicators of cytoplasmic calcium levels in higher plant cell protoplasts. Plant Physiol 90: 482–491

- Gilroy SG, Fricker MD, Read ND, Trewavas AJ (1991) Role of calcium in signal transduction of *Commelina* guard cells. Plant Cell 3: 333–344
- Glaasker E, Konings WN, Poolman B (1996) The application of pH sensitive fluorescent dyes in lactic acid bacteria reveals distinct extrusion systems for unmodified and conjugated dyes. Mol Membr Biol 13: 173–181
- Grabov A, Blatt MR (1997) Parallel control of the inward rectifier K⁺ channel by cytosolic free Ca²⁺ and pH in *Vicia* guard cells. Planta 201: 84–95
- Grabov A, Blatt MR (1998a) Membrane voltage initiates Ca²⁺ waves and potentiates Ca²⁺ increases with abscisic acid in stomatal guard cells. Proc Natl Acad Sci USA 95: 4778–4783
- Grabov A, Blatt MR (1998b) Co-ordination of signalling elements in guard cell ion channel control. J Exp Bot 49: 351–360
- Grabov A, Leung J, Giraudat J, Blatt MR (1997) Alteration of anion channel kinetics in wild type and *abi-1* transgenic *Nicotiona benthamiana* guard cells by abscisic acid. Plant J 12: 203–213
- Granados ME, Soriano E, Saavedra Molina A (1997) Use of pluronic acid F-127 with Fluo-3/AM probe to determine intracellular calcium changes elicited in bean protoplasts. Phytochem Anal 8: 204–208
- Grill E, Himmelbach A (1998) ABA signal transduction. Curr opin Plant Biol 1: 412–418
- Guern J, Mathieu Y, Thomine S, Jouanneau JP, Beloeil JC (1992) Plant cells counteract cytoplasmic pH changes but likely use these pH changes as secondary messages in signal perception. Curr Topics Plant Biochem Physiol 11: 249–269
- Hajnocky G, Thomas AP (1997) Minimal requirements for calcium oscillation driven by the IP₃ receptor. EMBO J 16: 3533–3543
- Hajnocky G, Robb-Gaspers LD, Seitz M, Thomas AP (1995) Decoding of cytosolic calcium oscillations in the mitochondria. Cell 82: 415–424
- Haugland RP (1996) Handbook of fluorescent probes and research chemicals, 6th edn. Molecular Probes Inc
- Haugland RP, Johnson ID (1999) Intracellular ion indicators. In:
 Mason WT (ed) Fluorescent and luminescent probes for bilogical activity, 2nd edn. Academic Press, San Diego, pp 40–50
- Heimovaara-Dijkstra S, Heistek JC, Wang M (1994) Counteractive effects of ABA and GA₃ on extracellular and intracellular pH and malate in barley aleurone. Plant Physiol 106: 359–365
- Heimovaara-Dijkstra S, Mundy J, Wang M (1995) The effect of intracellular pH on the regulation of the Rab 16 and the αamalyse 1/6-4 promoter by abscisic and gibberellic acid. Plant Mol Biol 27: 815–820
- Hinkle PM, Shanshala ED II, Nelson EJ (1992) Measurement of intracellular cadmium with fluorescent dyes. Further evidence for the role of calcium channels in cadmium uptake. J Biol Chem 267: 25553–25559
- Hodick D, Gilroy S, Fricker MD, Trewavas AJ (1991) Cytosolic Ca²⁺-concentrations and distributions in rhizoids of *Chara fragilis* Desv. determined by ratio analysis of the fluorescent probe indo-1. Bot Acta 104: 222–228
- Homolya L, Hollo Z, Germann UA, Pastan I, Gottesman MM, Sarkadi B (1993) fluorescent cellular indicators are extruded by the multidrug resistance protein. J Biol Chem 268: 21493–21496
- Hoth S, Dreyer I, Dietrich P, Becker D, Müller-Röber B, Hedrich R (1997) Molecular basis of plant-specific acid activation of K ⁺ uptake channels. Proc Natl Acad Sci USA 94: 4806–4810
- Hoyland J (1999) Fluorescent probes in practice potential artifacts. In: Mason WT (ed) Fluorescent and luminescent probes for biological activity, 2nd edn. Academic Press, San Diego, pp 108–113
- Inoué S (1990) Foundations of confocal scanned imaging light microscopy. In: Pawley JB (ed) Handbook of biological confocal microscopy, 2nd edn. Plenum, New York, pp 1–14
- Irving HR, Gehring CA, Parish RW (1992) Changes in cytosolic pH and calcium of guard cells precede stomatal movement. Proc Natl Acad Sci USA 89: 1790–1794

- Jabs T, Tschöpe M, Colling C, Hahlbrock K, Scheel D (1997) Elicitor-stimulated ion fluxes and O₂ from the oxidative burst are essential components in triggering defense gene activation and phytoalexin synthesis in parsley. Proc Natl Acad Sci USA 94: 4800–4805
- James-Kracke MR (1992) Quick and accurate method to convert BCECF fluorescence to pHi: calibration in three different types of cell preparations. J Cell Physiol 151: 596–603
- Johnson CH, Knight MR, Kondo T, Masson P, Sedbrook J, Haley A, Trewavas AJ (1995) Circadian oscillations in cytosolic and chloroplastic free calcium in luminous plants. Science 269: 1863–1865
- Kendall JM, Badminton MN, Dormer RL, Campbell AK (1994) Changes in free calcium in the endoplasmatic reticulum of living cells. Anal Biochem 221: 173–181
- Klein M, Martinoia E, Weissenbock G (1997) Transport of lucifer yellow CH into plant vacuoles evidence for direct energization of a sulphonated substance and implications for the design of new molecular probes. FEBS Lett 420: 86–92
- Klein M, Martinoia E, Weissenboeck G (1998) Directly energized uptake of β -estradiol 17-(β -glucuronide) in plant vacuoles is strongly stimulated by glutathione conjugates. J Biol Chem 273: 262–270
- Knight H, Knight MR (1995) Recombinant aequorin methods for intracellular calcium measurements in plants. Methods Cell Biol 49: 201–216
- Knight H, Trewavas AJ, Knight MR (1996) Cold calcium signaling in arabidopsis involves two cellular pools and a change in calcium signature after acclimation. Plant Cell 8: 489–503
- Knight H, Trewavas AJ, Knight MR (1997) Calcium signalling in Arabidopsis thaliana responding to drought and salinity. Plant J 12: 1067–1078
- Knight MR, Campbell AK, Smith SM, Trewavas AJ (1991) Transgenic plant aequorin reports the effects of touch and coldshock and elicitors on cytoplasmic calcium. Nature 352: 524–526
- Knight MR, Smith SM, Trewavas AJ (1992) Wind-induced plant motion immediately increases cytosolic calcium. Proc Natl Acad Sci USA 89: 4967–4977
- Knight MR, Read ND, Campbell AK, Trewavas AJ (1993) Imaging calcium dynamics in living plants using semi-synthetic recombinant aequorins. J Cell Biol 121: 83–90
- Kombrink E, Somssich IE (1995) Defense responses of plants to pathogens. Adv Bot Res 21: 1–34
- König K, Simon U, Halbhuber KJ (1996a) 3D resolved twophoton fluorescence microscopy of living cells using a modified confocal laser scanning microscope. Cell Mol Biol 42: 1181– 1194
- König K, So PTC, Mantulin WW, Tromberg BJ, Gratton E (1996b) Two-photon excited lifetime imaging of autofluorescence in cells during UVA and NIR photostress. J Microsc 183: 197–204
- König K, So PTC, Mantulin WW, Gratton E (1997) Cellular response to near-infrared femtosecond laser pulses in two-photon microscopes. Optics Lett 22: 135–136
- Kortje KH (1996) ESI contrast analysis: a new approach for element analysis with energy filtering transmission electron microscopy (EFTEM). J Microsc 184: 175–184
- Kropf DL, Henry CA, Gibbon BC (1995) Measurement and manipulation of cytosolic pH in polarizing zygotes. Eur J Cell Biol 68: 297–305
- Kuchitsu K, Yazaki Y, Sakano K, Shibuya N (1997) Transient cytoplasmic pH change and ion fluxes through the plasma membrane in suspension-cultured rice cells triggered by n-acetylchitooligosaccharide elicitor. Plant Cell Physiol 38: 1012–1018
- Kuhn MA, Hoyland B, Carter S, Zhang C, Haugland RP (1995) Fluorescent ion indicators for detecting heavy metals. Proc SPIE-Int Soc Opt Eng 2388: 238–244
- Lakowicz JR, Szmacinski H, Nowaczyk K, Johnson ML (1992) Fluorescence lifetime imaging of calcium using Quin-2. Cell Calcium 13: 131–147

- Lakowicz JR, Szmacinski H, Nowaczyk K, Lederer WJ, Kirby MS, Johnson ML (1994) Fluorescence lifetime imaging of intracellular calcium in COS cells using Quin-2. Cell Calcium 15: 7–27
- Lamb C, Dixon RA (1997) The oxidative burst in plant disease resistance. Annu Rev Plant Physiol Plant Mol Biol 48: 251–276
- Legué V, Blancaflor E, Wymer C, Perbal G, Fantin D, Gilroy S (1997) Cytoplasmic free Ca²⁺ in *Arabidopsis* roots changes in response to touch but not gravity. Plant Physiol 114: 789–800
- Lemtiri-Chlieh F, MacRobbie EAC (1994) Role of calcium in the modulation of *Vicia* guard cell potassium channels by abscisic acid: a patch clamp study. J Membr Biol 137: 99–107
- Leube MP, Grill E, Amrhein N (1998) ABI1 of *Arabidopsis* is a protein serine/threonine phosphatase highly regulated by the proton and magnesium concentration. FEBS Lett 424: 100–104
- Levine A, Tenhaken R, Dixon R, Lamb C (1994) H₂O₂ from the oxidative burst orchestrates the plant hypersensitive disease resistance response. Cell 79: 583–593
- Levine A, Pennel RI, Alvarez ME, Palmer R, Lamb C (1996) Calcium-mediated apoptosis in a plant hypersensitive response. Curr Biol 6: 427–437
- Linder B, Raschke K (1992) A slow anion channel in guard cells, activating at large hyperpolarization, may be principal for stomatal closing. FEBS Lett 313: 27–30
- Lipp P, Bootman MD (1999) High-resolution confocal imaging of elementary Ca²⁺ signals in living cells. In: Mason WT (ed) Fluorescent and luminescent probes for biological activity, 2nd edn. Academic Press, San Diego, pp 337–343
- Llopis J, McCaffery JM, Miyawaki A, Farquhar M, Tsien RY (1998) Measurement of cytosolic, mitochondrial and Golgi pH in single living cells with green fluorescent proteins. Proc Natl Acad Sci USA 95: 6803–6808
- Lynch J, Polito VS, Lauchli A (1989) Salinity stress increases cytoplasmic Ca²⁺ activity in maize root protoplasts. Plant Physiol 90: 1271–1274
- Malho R, Trewavas AJ (1996) Localized apical increases of cytosolic free calcium control pollen tube orientation. Plant Cell 8: 1935–1949
- Malho R, Read ND, Trewavas AJ, Pais MS (1995) Calcium channel activity during pollen tube growth and reorientation. Plant Cell 7: 1173–1184
- Mason WT, Dempster J, Hoyland J, McCann TJ, Somasundaram B,
 O'Brien W (1999) Quantitative digital imaging of biological activity in living cells with ion-sensitive fluorescent probes. In:
 Mason WT (ed) Fluorescent and luminescent probes for biological activity, 2nd edn. Academic Press, San Diego, pp 175–195
- Mathieu Y, Kurkdjian A, Xia H, Guern J, Koller A, Spiro MD, O'Neill M, Albersheim P, Darvill A (1991) Membrane responses induced by oligogalacturonides in suspension-cultured to-bacco cells. Plant J 1: 33–343
- Mathieu Y, Lapous D, Thomine S, Lauriere C, Guern J (1996a) Cytoplasmic acidification as an early phosphorylation-dependent response of tobacco cells to elicitors. Planta 199: 416–424
- Mathieu Y, Sanchez FJ, Droillard MJ, Lapous D, Lauriere C, Guern J (1996b) Involvement of protein phosphorylation in the early steps of transduction of the oligogalacturonide signal in tobacco cells. Plant Physiol Biochem 34: 399–408
- Mazars C, Thion L, Thuleau P, Graziana A, Knight, Moreau M, Ranjeva R (1997) Organization of cytoskeleton controls the changes in cytosolic calcium of cold-shocked *Nicotiana plumbaginifolia* protoplasts. Cell Calcium 22: 413–420
- McAinsh MR, Brownlee C, Hetherington AM (1992) Visualizing changes in cytosolic-free Ca²⁺ during the response of stomatal guard cells to abscisic acid. Plant Cell 4: 1113–1122
- McAinsh MR, Webb AAR, Taylor JE, Hetherington AM (1995) Stimulus-induced oscillations in guard cell cytosolic free calcium. Plant Cell 7: 1207–1219
- McAinsh MR, Brownlee, Hetherington AM (1997) Calcium ions as second messengers in guard cell signalling. Physiol Plant 100: 16–29

- Miller AL, Karplus E, Jaffe LF (1994) Imaging [Ca²⁺] with aequorin using a photon imaging detector. Methods Cell Biol 40: 305–338
- Miyawaki A, Llopis J, Heim R, McCaffery JM, Adams JA, Ikura M, Tsien RY (1997) Fluorescent indicators for Ca²⁺ based on green fluorescent proteins and calmodulin. Nature 388: 882–887
- Monck JR, Oberhauser AF, Keating TJ, Fernandez JM (1992) Thin-section ratiometric Ca²⁺ images obtained by optical sectioning of fura-2 loaded mast cells. J Cell Biol 116: 745–759
- Muhling KH, Sattelmacher B (1997) Determination of apoplastic K^+ in intact leaves by ratio imaging of PBFI-fluorescence. J Exp Bot 48: 1609–1614
- Muir SR, Sanders D (1996) Pharmacology of Ca²⁺ release from red beet microsomes suggests the presence of ryanodine receptor homologs in higher plants. FEBS Lett 395: 39–42
- Neher E, Augustine GJ (1992) Calcium gradients and buffers in bovine chromaffin cells. J Physiol 450: 273–301
- Nuccitelli R, ed (1994) A practical guide to the study of calcium in living cells. Methods Cell Biol, vol 40
- Okazaki Y, Kikuyama M, Hiramoto Y, Iwasaki N (1996) Shortterm regulation of cytosolic Ca²⁺, cytosolic pH and vacuolar pH under NaCl stress in the charophyte alga *Nitellopsis obtusa*. Plant Cell Environ 19: 569–576
- Opas M (1997) Measurement of intracellular pH and pCa with a confocal microscope. Trends Cell Biol 7: 75–80
- Owen C (1992) Comparison of spectrum-shifting intracellular pH probes 5' (and 6')-carboxy-10-dimethylamino-3-hydroxy-spiro[7H-benzo[c]xanthene-7,1'(3'H)-isobenzofuran]-3'-one and 2',7'-biscarboxyethyl-5(and 6)-carboxyfluorescein. Anal Biochem 204: 65–71
- Owen CS, Wahl ML, Leeper DB, Perry HD, Bobyock SB, Russell M, Woodward W (1995) Accurate whole-spectrum measurements of intracellular pH and [Na⁺]. J Fluoresc 5: 329–335
- Parton RM, Fischer S, Malho R, Papasouliotis O, Jelitto TC, Leonard T, Read ND (1997) Pronounced cytoplasmic pH gradients are not required for tip growth in plant and fungal cells. J Cell Sci 110: 1187–1198
- Pierson ES, Miller DD, Callaham DA, Van-Aken J, Hackett G, Hepler PK (1996) Tip-localized calcium entry fluctuates during pollen tube growth. Dev Biol 174: 160–173
- Piñeros M, Tester M (1995) Characterization of a voltage-dependent Ca²⁺ selective channel from wheat roots. Planta 195: 478–488
- Plieth C, Sattelmacher B, Hansen UP, Thiel G (1998) The action potential in *Chara*: Ca²⁺ release from internal stores visualized by Mn²⁺-induced quenching of furadextran Plant J 13: 167–175
- Pőnitz J, Roos W (1994) A glucose-activated electron transfer system in the plasma membrane stimulates the H⁺-ATPase in *Penicillum cyclopium*. J Bacteriol 176: 5429–5438
- Price AH, Taylor A, Ripley SJ, Griffiths A, Trewavas AJ, Knight MR (1994) Oxidative signals in tobacco increase cytosolic calcium. Plant Cell 6: 1301–1310
- Rea PA, Li ZS, Lu YP, Drozdowicz YM, Martinoia E (1998) From vacuolar GS-X pumps to multispecific abc transporters. Annu Rev Plant Physiol Plant Mol Biol 49: 727–760
- Reid RJ, Smith FA, Whittington J (1989) Control of intracellular pH in *Chara corallina* during uptake of weak acid. J Exp Bot 40: 883–891
- Riondet C, Cachon R, Wache Y, Alcaraz G, Divies C (1997) Measurement of the intracellular pH in *Escherichia coli* with the internally conjugated fluorescent probe 5-(and 6-)carboxyfluorescein succinimidyl ester. Biotechnol Tech 11: 735–738
- Rizzuto R, Simpson AWM, Brini M, Pozzan T (1993) Rapid changes of mitochondrial Ca²⁺ revealed by specifically targeted recombinant aequorin. Nature 358: 325–327
- Roos W (1992) Confocal pH topography in plant cells acidic layers in the peripheral cytoplasm and the apoplast. Bot Acta 105: 253–259
- Roos W, Slavík J (1987) Intracellular pH topography of *Penicillium cyclopium* protoplasts. Maintenance of ΔpH by both passive and active mechanisms. Biochim Biophys Acta 899: 67–75

- Roos W, Evers S, Hieke M, Tschöpe M, Schumann B (1998) Shifts of the intracellular pH distribution as a part of the signal mechanism leading to the elicitation of benzophenanthridine alkaloids in cultured cells of *Eschscholtzia californica*. Plant Physiol 118: 349–364
- Russ U, Grolig F, Wagner G (1991) Changes of cytoplasmic free Ca²⁺ in the green alga *Mougeotia scalaris* as monitored with Indo-1 and their effect on the velocity of chloroplast movements. Planta 184: 105–112
- Sako Y, Sekihata A, Yanagisawa Y, Yamamota M,
 Shimada Y, Ozaki K, Kusumi A (1997) Comparison of two-photon excitation laser scanning microscopy with UV-confocal laser scanning microscopy in three-dimensional calcium imaging using the fluorescence indicator Indo-1. J Microsc 185: 9–20
- Sanders R, Gerritsen HC, Draaijer A, Houpt PM, Levine YK (1994) Fluorescence lifetime imaging of free calcium in single cells. Bioimaging 2: 131–138
- Scalettar BA, Swedlow JR, Sedat JW, Agard DA (1996) Dispersion, aberration and deconvolution in multi-wavelength fluorescence images. J Microsc 182: 50–60
- Schild D (1996) Laser scanning microscopy and calcium imaging. Cell Calcium 19: 281–296
- Schroeder JI, Hagiwara S (1990) Repetitive increases in cytosolic Ca²⁺ of guard cells by abscisic acid activation of non-selective Ca²⁺ permeable channels. Proc Natl Acad Sci USA 87: 9305–9309
- Schulz-Lessdorf B, Hedrich R (1995) Protons and calcium modulate SV-type channels in the vacuolar-lysosomal compartment channel interaction with calmodulin inhibitors. Planta 197: 655–671
- Sedbrook JC, Kronebusch PJ, Borisy CG, Trewavas AJ, Masson PH (1996) Transgenic aequorin reveals organ-specific cytosolic Ca²⁺ responses to anoxia in *Arabidopsis thaliana* seedlings. Plant Physiol 111: 243–257
- Seksek O, Henry-Toulme N, Sureau F, Bolard J (1991) SNARF-1 as an intracellular pH indicator in laser microspectrofluorometry: a critical assessment. Anal Biochem 193: 49–54
- Seksek O, Biwersi J, Verkman AS (1995) Direct measurement of trans-Golgi pH in living cells and regulation by second messengers. J Biol Chem 270: 4967–4970
- Shabala SN, Newman IA, Morris J (1997) Oscillations in H⁺ and Ca²⁺ ion fluxes around the elongation region of corn roots and effects of external pH. Plant Phys 113: 111–118
- Shimomura O (1991) Preparation and handling of aequorin solutions for the measurement of cellular Ca²⁺. Cell Calcium 12: 635–642
- Shimomura O, Musicki B, Kishi Y (1988) Semi-synthetic aequorins. Biochem J 251: 405–410
- Shorte SL, Bolsover S (1999) Imaging reality: understanding maps of physiological cell signals measured by fluorescence microscopy and digital imaging. In: Mason WT (ed) Fluorescent and luminescent probes for biological activity, 2nd edn. Academic Press, San Diego, pp 94–107
- Slavik J, Kotyk A (1984) Intracellular pH distribution and transmembrane pH profile of yeast cells. Biochim Biophys Acta 766: 679–684
- Slayman CL, Moussatos VV, Webb WW (1994) Endosomal accumulation of pH indicator dyes delivered as acetoxymethyl esters. J Exp Biol 196: 419–438
- Speksnijder J, Miller AL, Weisenseel MH, Chen TH, Jaffe LF (1989) Calcium buffer injections block fucoid egg development by facilitating calcium diffusion. Proc Natl Acad Sci USA 86: 6607–6611
- Staxén I, Pical C, Montgomery LT, Gray JE, Hetherington AM, McAinsh MR (1999) Abscisic acid induces oscillations in guard-cell cytosolic free calcium that involve phosphoinositide-specific phospholipase C. Proc Natl Acad Sci USA 96: 1779–1784
- Swanson SJ, Jones RL (1996) Gibberellic acid induces vacuolar acidification in barley aleurone. Plant Cell 8: 2211–2221

- Szmacinski H, Lakowicz JR (1995a) Fluorescence lifetime-based sensing and imaging. Sensors Actuators 29: 16–24
- Szmacinski H, Lakowicz JR (1995b) Possibility of simultaneously measuring low and high calcium concentrations using Fura-2 and lifetime-based sensing. Cell Calcium 18: 64–75
- Szmacinski H, Lakowicz JR (1996) Fluorescence lifetime characterization of magnesium probes: improvement of Mg²⁺ dynamic range and sensitivity using phase-modulation fluorometry. J Fluoresc 6: 83–95
- Szmacinski H, Lakowicz R (1997) Sodium green as a potential probe for intracellular sodium imaging based on fluorescence lifetime. Anal Biochem 250: 131–138
- Szmacinski H, Gryczinski I, Lakowicz JR (1993) Calcium-dependent fluorescence of indo-1 for one- and two-photon excitation of fluorescence. Photochem Photobiol 58: 341–345
- Taylor A, Manison N, Brownlee C (1997) Regulation of channel activity underlying cell volume and polarity signals in *Fucus*. J Exp Bot 48: 579–588
- Taylor DP, Slattery J, Leopold AC (1996) Apoplastic pH in corn root gravitropism: a laser scanning confocal microscopy measurement. Physiol Plant 97: 35–38
- Tazawa M, Shimada K, Kikuyama M (1995) Cytoplasmic hydration triggers a transient increase in cytoplasmic Ca²⁺ concentration in *Nitella flexilis*. Plant Cell Physiol 36: 335–340
- Thiel G, MacRobbie EAC, Blatt MR (1992) Membrane transport in stomatal guard cells: the importance of voltage control. J Membr Biol 126: 1–18
- Thiel G, Blatt MR, Fricker MD, White IR, Millner P (1993) Modulation of K + channels in *Vicia* stomatal guard cells by peptide homologs to the auxin-binding protein C terminus. Proc Natl Acad Sci USA 90: 11493–11497
- Thomas JA, Buchsbaum RN, Zimniak A, Racker E (1979) Intracellular pH measurements in Ehrlich aszites tumor cells utilizing spectroscopic probes generated in situ. Biochemistry 18: 2210–2216
- Thuleau P, Ward JM, Ranjeva R, Schroeder JI (1994) Voltagedependent calcium-permeable channels in the plasma membrane of a higher plant cell. EMBO J 13: 2970–2975
- Tommasini R, Martinoia E, Grill E, Dietz KJ, Amrhein N (1993) Transport of oxidized glutathione into barley vacuoles: evidence for the involvement of the glutathione-S-conjugate ATPase. Z Naturforsch 48c: 867–871
- Trewavas AJ, Malhó R (1997) Signal perception and transduction: the origin of the phenotype. Plant Cell 9: 1181–1195
- Trewavas AJ, Malhó R (1998) Ca²⁺ signalling in plant cells: the big network! Curr Opin Plant Biol 1: 428–433
- Tsien RY (1980) New calcium indicators and buffers with high selectivity against magnesium and protons: design, synthesis, and properties of prototype structures. Biochemistry 19: 2396–2404
- Tsien RY (1989) Fluorescent indicators of ion concentrations. Methods Cell Biol 30: 127–156
- Vamos S, Welling LW, Wiegmann B (1997) Fluorescent analysis in polarized MDCK cell monolayers: intracellular pH and calcium interactions after apical and basolateral stimulation with arginine vasopressin. Cell Calcium 19: 307–314
- Van der Zee J, Mason RP, Eling TE (1989) The oxidation of the calcium probe Quin2 and its analogs by prostaglandin H synthase. Arch Biochem Biophys 271: 64–71
- Ward JM, Pei ZM, Schroeder JI (1995) Roles of ion channels in initiation of signal transduction in higher plants. Plant Cell 7: 833–844
- Webb AAR, McAinsh MR, Mansfield TA, Hetherington AM (1996) Carbon dioxide induces increases in guard cell cytosolic free calcium. Plant J 9: 297–304
- White NS, Errington RJ, Fricker MD, Wood JL (1996) Aberration control in quantitative imaging of botanical specimens by multidimensional fluorescence microscopy. J Microsc 181: 99–116
- Williams DA, Cody SH, Dubbin PN (1993) Introducing and calibrating fluorescent probes in cells and organelles. In: Mason

- WT (ed) Fluorescent and luminescent probes for biological activity. Academic Press, London, pp 321–334
- Wolniak SM, Bart KM (1985) The buffering of calcium with quin2 reversibly forestalls anaphase onset in stamen hair cells of *Tradescantia*. Eur J Cell Biol 39: 33–40
- Wu Y, Kuzma J, Marechal E, Graeff R, Lee HC, Foster R, Chua NH (1997) Abscisic acid signaling through cyclic ADP-ribose in plants. Science 278: 2126–2130
- Wymer CL, Bibikova TN, Gilroy S (1997) Cytoplasmic free calcium distributions during the development of root hairs of *Arabidopsis thaliana*. Plant J 12: 427–439
- Yassine M, Salmon JM, Vigo J, Viallet P (1997) cSNARF-1 as a pH_i fluoroprobe: discrepancies between conventional and

- intracellular data do not result from protein interactions. J Photochem Photobiol 37: 18–25
- Yazaki Y, Asukagawa N, Ishikawa Y, Ohta E, Sakata M (1988) Estimation of cytoplasmic free Mg²⁺ levels and phosphorylation potentials in mung bean root tips by in vivo ³¹P NMR spectroscopy. Plant Cell Physiol 29: 919–924
- Zhang WH, Rengel Z, Kuo J (1998) Determination of intracellular Ca²⁺ of intact wheat roots: loading of acetoxymethyl ester of fluo-3 under low temperature. Plant J 15: 147–151
- Zimmermann S, Nürnberger T, Frachisse JM, Wirtz W, Guern J, Hedrich R, Scheel D (1997) Receptor-mediated activation of a plant Ca²⁺ permeable ion channel involved in pathogen defense. Plant Biol 94: 2751–2755